Environmental Science Advances

Accepted Manuscript

This article can be cited before page numbers have been issued, to do this please use: V. R. Ferreira and M. Azenha, *Environ. Sci.: Adv.*, 2024, DOI: 10.1039/D4VA00230J.

ROYAL SOCIETY OF CHEMISTRY

rsc.li/esadvances

View Article Online
DOI: 10.1039/D4VA00230J

Environmental Significance Statement

Visible light-driven micro/nanomotors (Vis-LDM) represent a promising avenue for ecological and efficient self-propulsion. Visible light is abundant, clean, and controllable, offering low cost and ease of use, making Vis-LDM ideal for tasks like environmental remediation. Recent studies focus on Vis-LDM for environmental pollutant removal by photocatalysis, highlighting their potential to degrade organic pollutants effectively. The review of research in this field, especially those published from 2020 to 2024, addresses the need to summarize and organize the existing knowledge. This will facilitate scientific and technological advancements, providing a comprehensive overview of materials, synthesis methods, recent innovations, and challenges. Such efforts aim to establish a solid foundation for future research, enhancing the application of Vis-LDM in environmental pollutant photocatalysis and contributing to more sustainable environmental practices.

View Article Online
DOI: 10.1039/D4VA00230J

Advancements in Visible Light-Driven Micro/nanomotors for Photodegradation of Environmental Pollutants

Authors:

Vanessa R. Ferreira and Manuel Azenha+

Affiliations:

CIQUP/IMS, Department of Chemistry and Biochemistry, Faculty of Sciences, University of Porto, Rua do Campo Alegre s/n, 4169-007 Porto, Portugal

View Article Online
DOI: 10.1039/D4VA00230J

Advancements in Visible Light-Driven Micro/nanomotors for Photodegradation of Environmental Pollutants

Abstract

Visible light-driven motors (Vis-LDM) have shown significant potential for water decontamination processes through the synergistic interaction between their active movement and photocatalytic properties, enabling more efficient degradation of organic pollutants. This review highlights recent advances in Vis-LDM photocatalysts for sustainable environmental pollution mitigation. Innovations include fuelless Vis-LDM with hybrid structures and crystalline materials, and biofuel alternatives like water and glucose, though logistical challenges persist. The use of natural materials like lignin and cellulose nanocrystals promotes sustainability but faces energy conversion efficiency challenges. Strategies to enhance efficiency, such as doping and heterojunction formation, are discussed. Advances in stability, reuse, and magnetic recovery capabilities are also reviewed. Collective behavior and environmental adaptability are explored to improve catalytic efficiency. Despite the presented advances, definitive solutions to these limitations have not yet been found. A perspective on the directions for future research is also included in this review, namely the need to resolve issues of scalability, cost-effectiveness, and environmental compatibility. Additionally, investing in Vis-LDM with programmable routes and precise navigation can enhance versatility and accuracy. Selective behavior to target hazardous contaminants is important; the molecular imprinting technique being a potential solution. Future research should also focus on real-world testing and navigation improvements. Overcoming these challenges is essential to fully harness the potential of Vis-LDM for environmental remediation and global environmental health.

Keywords: *Visible light-driven motors; Self-propulsion; Photodegradation; Environmental pollutants; Sustainability*

1. Introduction

Micro/nanomotors are devices capable of autonomously moving in unstirred liquid environments through catalytic reactions or external stimuli (1), enabling them as useful devices for applications in environmental remediation (2,3), encompassing monitoring and cleaning of aquatic and terrestrial environments, and also in biomedicine (4,5), such as targeted drug delivery, diagnostics, and therapies. The mobility of these motors is facilitated by various mechanisms, one of which involves morphological asymmetry. This asymmetry is often created by metal deposition on one side, forming two distinct hemispheres. This design, commonly referred to as Janus structure, enables movement generation by creating chemical or thermal gradients (6). Additionally, other mechanisms contribute to the autonomous motion of micro/nanomotors. These include catalytic reactions, where the

View Article Online
DOI: 10.1039/D4VA00230J

motors surface interacts with specific reactants to produce propulsion; light-induced propulsion through photothermal or photocatalytic effects; and manipulation by magnetic or electric fields (5,7–11). These diverse propulsion mechanisms enhance the versatility and applicability of these motors in different environments and tasks (1).

Studies on micro/nanomotors are classified into five categories based on the type of energy used: chemical fuels, magnetic fields, electric fields, ultrasound, and light (12). Motors powered by chemical fuels, such as H_2O_2, generate bubbles or chemical gradients to move. These motors face challenges of motion control and toxicity due to the catalytic decomposition of H_2O_2 into O_2 and H_2O, leading to uncontrolled autonomous motion (7). Electric motors use electric gradients to move, but their application is generally restricted to two-dimensional movements (8). Ultrasound provides robust propulsion but requires sophisticated equipment (9). Magnetic micromotors use magnetic fields for propulsion and control, allowing precise manipulation in liquids. Made from ferromagnetic materials, they are ideal for applications like targeted drug delivery and contaminant removal due to their remote controllability. However, their effectiveness can be limited by the strength of the magnetic field required and challenges in complex environments. (11). Light-driven motors, especially those driven by visible light, have gained emphasis due to advantages such as low cost, ease of control, and the ability to perform complex tasks (5). Visible light is an abundant, clean, and controllable energy source, making it promising for various applications such as detection, biomedicine, and environmental remediation (1). The particularity of being able to move under visible light offers an ecological and efficient propulsion method, with potential applications in microscopic cargo transport and complex tasks (10).

Focusing on visible light-driven motors (Vis-LDM), this may present different propulsion mechanisms, with the most described in the literature being the autophoresis , autoelectrophoresis, autodiffusiophoresis and bubble propulsion (12). In autophoresis, light increases the temperature in a specific region of the motor, creating a thermal gradient that generates movement. Heat-sensitive materials, such as certain metals and semiconductors, respond to temperature changes by expanding or contracting, resulting in a force that moves the motor (13). In autoelectrophoresis, light generates an electric field around charged particles, resulting from photocatalytic reactions on the motors surface (14). This electric field induces the movement of charged particles, creating a propulsion effect (15). In bubble propulsion, light hits motors causing photolysis and the release of gas that accumulates as bubbles on the motors surface (16). The expulsion of bubbles generates the impulse that moves the motor in the opposite direction (17). In autodiffusiophoresis, light creates chemical gradients around particles, activating chemical reactions that result in concentration differences. These gradients induce directional movements of particles based on diffusion forces (18,19).

Vis-LDM, compared to static photocatalytic systems operated under magnetic stirring, offer the advantage of higher catalytic efficiency due to improved mixing of reactants. These motors can be employed in dynamic applications, such as pollutant removal, with simple

View Article Online
DOI: 10.1039/D4VA00230J

light irradiation. Furthermore, with advanced design, it is possible to control the direction and speed of movement. However, these motors are complex to design and manufacture, can be sensitive to environmental conditions, and have limitations regarding the available energy for movement. Scaling up for large-scale use is challenging due to the complexity of fabrication and control (20). On the other hand, static photocatalytic systems are simpler to scale for industrial processes, such as water treatment, due to their straightforward design. They provide greater stability and durability as they do not suffer mechanical wear and have reduced maintenance costs. However, these systems exhibit reduced efficiency due to the lack of movement, which limits reactant mixing, as evidenced by some studies (21,22).They are less effective in dynamic environments and rely on appropriate lighting conditions, making them more suitable for stationary applications.

The literature review methodology, followed to structure this review, considered a search conducted in major databases, such as Web of Science, PubMed and Scopus. The research was conducted in phases to reach the final topic. In the first phase, all publications, including patents, released over the past 10 years (2014-2024) were searched using the keywords "micromotor,"OR "nanomotor,"OR "microswimmer," OR "nanoswimmer." This initial search yielded 2100 articles, of which 175 were relevant to environmental remediation, identified by applying additional keywords ("Photodegradation" OR "Pollutant Degradation" OR "Environmental Remediation"). 39 of the articles were review articles, which revealled a growing interest in these devices for environmental remediation in recent years, with more than 2/3 of the reviews (27) published in the last 5 years. When the search was further restricted to "visible light-driven" AND (micromotor OR nanomotor OR microswimmer OR nanoswimmer)" AND ("Photodegradation" OR "Pollutant Degradation" OR "Environmental Remediation"), only 2 reviews were found. One of these reviews included only a small subsection on the topic, with the last comprehensive review published in 2020 (23), highlighting the emergent nature of this research area.

Hence, the review of the research on Vis-LDM applied to environmental pollutant removal by photocatalysis was motivated by the absence of bibliographic reviews after 2020 on this specific topic. This literary gap justifies the urge to organize and synthesize the available information, facilitating scientific and technological advancement in this promising area. To structure the available literature, the following inclusion and combined rules were applied:

- Studies on Vis-LDM photocatalysts, regardless of format and size.
- Studies demonstrating photocatalytic capacity in the degradation of organic pollutants.
- Literature published in the period 2020-June 2024.

Based on the latest reviews on visible light-driven motors and environmental remediation (23–26), the main advantages and limitations of these devices in the context of pollutant photodegradation have been identified. This review focuses on the primary adaptations made to Vis-LDMs over the past four years to address these identified limitations, with a continuous emphasis on enhancing photocatalytic performance for pollutant degradation. The review presents and discusses the main development in the field of Vis-LDM, offering

View Article Online
DOI: 10.1039/D4VA00230J

a comprehensive overview of materials, synthesis methods, and the challenges to be overcome for the efficient application of Vis-LDM in environmental pollutant photocatalysis.

2. Vis-LDM photocatalysts: materials and methods

The essence of Vis-LDM photocatalysts lies in utilizing energy from visible radiation to generate photoexcited e^+/h^- pairs that activate oxidation-reduction reactions, while employing this energy for self-propulsion (24). The most commonly used photocatalysts for Vis-LDM applications combine good absorption of visible light, efficient charge separation, and high chemical stability. Considering this, the choice of photocatalytic materials to use as well as the synthesis methods are important for the preparation of photocatalytic Vis-LDM.

2.1 Photocatalytic materials

Among the materials most studied and utilized up to 2020 were gC_3N_4, $BiVO_4$, CdS, WO_3, and MoS_2, due to their favorable properties and potential for various applications, especially in pollutant degradation (23). More recently, photocatalysts with narrow bandgaps, which demonstrate a capacity for absorption and response to visible light, such as Ag_3PO_4 (≈2.45 eV), BiOI (≈1.7 eV), Cu_2O (≈2.1 eV), and gC_3N_4 (≈2.7 eV), will be tested for obtained Vis-LDM. Table 1 summarizes the most recently explored photocatalysts, highlighting their beneficial characteristics and limitations, along with possible strategies to overcome these limitations.

Graphitic carbon nitride (gC_3N_4)

The gC_3N_4 is an active catalyst under visible light, which has attracted considerable interest for various environmental applications in the past decade (27). Its advantages include being a non-metallic material, being active under visible light, and being easily synthesized. Vis-LDM based on gC_3N_4 have demonstrated excellent performance as propellers in aqueous media, using very low concentrations of H_2O_2 or even without H_2O_2 under visible light. These micromotors mostly utilize a bubble propulsion mechanism, associated especially with the spherical and tubular forms of gC_3N_4, for the removal of organic contaminants in water (28). Additionally, gC_3N_4 stands out for its chemical and thermal stability, as well as being eco-friendly, non-toxic, and biodegradable, suitable for water treatment and air purification. However, rapid e^+/h^- pair recombination and insufficient efficiency in charge separation and transfer were the main limitations identified in its application as a Vis-LDM photocatalyst (29). The most recent strategies explored to overcome these limitations focus on structural modifications, both morphologically and on the surface, associated with doping and heterojunction processes (30–32) (strategies explored in section 4.2).

View Article Online
DOI: 10.1039/D4VA00230J

Copper (I) oxide (Cu_2O)

The Cu_2O was predominantly described for the preparation of photocatalytic Vis-LDM with asymmetric structures (33), forming heterostructures with other conductors/semiconductors (13,34). Although Cu_2O has potential as a photocatalyst in Vis-LDM, the main limitations identified include limited photocatalytic efficiency, low chemical stability, and sensitivity to visible light which, if excessive, reduces the useful lifetime of the photocatalyst as it promotes its self-destruction. In recent years, the introduction of defects and control of crystal facets (35) have been among the main surface modifications studied to address these limitations, considering the important physicochemical crystalline properties of Cu_2O (36) (strategies explored in section 4.2.2).

Silver phosphate (Ag_3PO_4)

The Ag_3PO_4 is considered a promising photocatalyst, regarded as one of the semiconductors with the highest photocatalytic activities under visible light, being effective in degrading a wide range of organic pollutants (21,37,38). The crystalline structure of Ag_3PO_4 favors efficient separation of e^+/h^- pairs, minimizing recombination and maximizing photocatalytic efficiency. Additionally, Ag_3PO_4 is highly effective in generating highly reactive free radicals, such as hydroxyl radicals, which are crucial for contaminant degradation. However, the photocatalysis by Vis-LDM based on Ag_3PO_4 remains at the laboratory scale due to its uncontrollable photocorrosion and high cost (39). To improve stability and efficiency, recent modifications explored the doping with other metals, forming composites, or incorporating Ag_3PO_4 into support matrices, (29,40) (examples discussed in section 4.2.2).

Bismuth oxyiodide (BiOI)

Less explored is BiOI, another visible light-excited semiconductor with studied photocatalytic activity for pollutant degradation. Due to its layered structure, BiOI exhibits efficient e^+/h^- pair separation, resulting in high photocatalytic activity for the degradation of organic pollutants (41). Additionally, it shows good chemical stability in aqueous and oxidizing conditions, which is beneficial for water treatment applications (42). However, its photocatalytic activity has been described as limited due to low electrical conductivity, and slow hole transfer kinetics (25,43). Recently, attempts have been made to address some of these limiting issues primarily through morphology control (44–48) (examples discussed in sections 4.2.2 and 4.3), forming heterojunctions, doping, or adjusting the composition of BiOI.

High bandgap (UV range) photocatalysts

View Article Online
DOI: 10.1039/D4VA00230J

In addition to low bandgap photocatalysts, higher bandgap photocatalysts such as TiO_2 and ZnO have also been explored for the synthesis of visible light-driven micromotors (Vis-LDM), leveraging their excellent photocatalytic properties. Various strategies have been investigated to enhance the light absorption capacity of semiconductor-based micromotors with high bandgaps suitable for the visible light spectrum. These strategies include integrating photocatalysts capable of absorbing visible light through p-n junctions (49,50), employing surface doping techniques (51,52), and utilizing dye sensitization methods (53).

Doping is an effective technique to adjust the bandgap energy of high-band-gap photocatalysts, making them more responsive to visible light. This technique introduces new energy levels within the materials bandgap, modifying the band structure to allow electrons to be excited by lower energy photons (54). Additionally, dopants can create defects in the materials crystalline structure, such as oxygen vacancies, which act as capture centers for electrons or holes, decreasing the excitation energy. Doping can also alter the width and position of the valence and conduction bands through crystal lattice distortion or changes in the materials bonding chemistry (55). Finally, the presence of dopants can induce local polarizations within the crystalline lattice, altering the charge distribution and local potentials, modifying the bandgap structure (56). The interest in doping highly active photocatalysts, such as TiO_2 and ZnO, to obtain Vis-LDM has remained high. Noble metals to be the most common dopants due to several advantages, namely the high catalytic activity achieved and easy incorporation into the photocatalyst structure during the doping process (55). Moreover, they improve charge separation by acting as charge capture centers, facilitating efficient separation of electrons and holes generated during the photocatalytic process. Light absorption is also enhanced, especially in the case of noble metals as Au and Ag, which exhibit plasmonic properties, contributing to greater light absorption by the photocatalyst (57). Lastly, noble metals offer chemical stability, which is crucial to ensure the long-term durability and efficiency of doped photocatalysts (51).

The formation of heterojunctions, combining two distinct semiconductors, is an effective technique for spatial separation of photogenerated e^+/h^- pairs (49,58–60). When semiconductors have different Fermi energy levels, an embedded electric field develops at the interface due to the spontaneous diffusion of electrons from the higher Fermi semiconductor to the lower one. Upon light exposure, electrons and holes can move between the semiconductors through this electric field, reducing recombination. The formation of the electric field and carrier transfer depends on factors such as semiconductor conductivity, work function, and band potentials (61). Gibbs and collaborators (50) combined TiO_2 (n-type) and CuO_2 (p-type) semiconductors to create hybrid Vis-LDM using electron beam evaporation on SiO_2 microspheres. In this study, a p-type semiconductor (CuO_2) was combined with an n-type semiconductor (TiO_2) to modify the electrical conductivity of the hybrid photocatalyst. The use of TiO_2 introduced a small amount of impurity into the CuO_2 crystalline structure, modifying its electronic properties and reducing the bandgap. A

View Article Online
DOI: 10.1039/D4VA00230J

potential barrier formed at the CuO_2-TiO_2 junction, creating an internal electric field that prevents electron-hole recombination, thereby increasing photocatalytic efficiency (Figure 1). This strategy can be applied to other semiconductors, such as ZnO, and offers a more economical approach since it does not require noble metals commonly used in efficient Vis-LDM production.

Figure 1. Representative scheme: a) of Vis-LDM and b) about charge transfer in a heterostructure with a p–n junction. Reproduced with permission from (50) (Copyright © 2020 WILEY-VCH).

Organic dye sensitization also allows for the reduction of a high bandgap photocatalyst bandgap, enabling visible light absorption. This is achieved by impregnating dyes onto the photocatalysts surface, enabling it to absorb visible light photons that it previously could not (62). This sensitizing dyes must present several conditions to optimize photocatalytic activity under visible light. Firstly, they must strongly absorb within the visible light range (400-700 nm) in order to have a high molar extinction coefficient that guarantees significant light absorption. Chemical and photochemical stability is crucial to resist photodegradation during photocatalysis. They must bind strongly to the photocatalyst surface and be chemically compatible to avoid adverse reactions. The other essential parameter is to possess the ability to efficiently transfer excited electrons to the photocatalysts conduction band, as is their effectiveness in charge separation to minimize e^+/h^- recombination (63). Zheng et al. (53) demonstrated the use of Vis-LDM nanotrees based on Si/TiO_2. Dyes with different sensitivities to visible light (green, red, and blue) were incorporated into the nanotree surfaces to control the nanomotors movement according to the irradiated light source. (Figure 2a) Groups of Si/TiO2 nanomotors with N719, D5, and SQ2 were created, each absorbing visible light in a specific range. Under blue or red visible light, the groups with SQ2 and D5 were activated, exhibiting movements controlled by the corresponding light source. The nanomotors with SQ2 (red) and D5 (blue) exhibited spontaneous and different trajectories under blue and red light, respectively (Figure 2b)

Figure 2. Representation of: (a)dye-sensitized nanotree, activated by a photoelectrochemical reaction with numerically simulated charge distribution (displayed in a color map); (b) movement generated by nanotrees sensitized with the dyes D5 and SQ2 under alternating illumination of blue light (475 nm) and red light (660 nm). (Include the molecular structures of the dyes D5 and SQ2). Adapted from (53) Licensed under an open-access Creative Commons CC BY 4.0 license).

The intensive research conducted since 2020 into the modification of some of the previously mentioned materials to address their limitations will be focused in section 4.1.

2.2 Synthesis methods

View Article Online
DOI: 10.1039/D4VA00230J

The synthesis of Vis-LDM typically involves different methods to enhance their light absorption capabilities and photocatalytic efficiency, being the most cited the sol gel method (64–66); hydrothermal/solvothermal method (16,31,53,67) and electrochemical method (68,69), as summarized in Table 1. The sol-gel process is widely used for synthesizing Vis-LDM based on semiconductor materials and make it possible to obtain motors with high surface areas and controlled porosity. In this method, metal alkoxides or metal salts are hydrolyzed and condensed to form a gel, which is then dried and calcined to obtain the desired oxide material (23). The hydrothermal/solvothermal method involve the crystallization of substances from high-temperature aqueous or solvent solutions under high pressure, for obtaining Vis-LDM. By controlling the reaction parameters such as temperature, time, and solvent, nanostructured materials with tailored properties can be synthesized. This method is associated with the synthesis of amorphous or spherical Vis-LDM, morphology as commonly described in the literature (24). The electrochemical method, particularly anodic oxidation, is associated with the preparation of Vis-LDM with tube form, by electrochemically oxidizing a metal substrate in an electrolyte solution (70). The setup includes a metal working electrode, an inert counter electrode, and an electrolyte containing fluoride ions. Parameters like voltage, time, and temperature control the nanotube dimensions. Post-treatment steps such as rinsing and annealing improve their properties. This method is simple, cost-effective, and scalable, making it ideal for applications in photocatalysis, energy storage, sensors, and biomedical fields (56).

Regarding the preparation of Janus structures, widely studied for achieving more efficient and directional self-propulsion, chemical vapor deposition (CVD) and electrodeposition (ED) methods are the most commonly described in the literature. The PVD technique is used to uniformly deposit thin films on substrates by vaporizing the target material and depositing it in a controlled manner. PVD can be generally divided into two sub-techniques: conventional PVD and glancing angle deposition (GLAD). Conventional PVD, widely associated with the sputtering technique, is the most common approach for synthesizing Vis-LDM, allowing the deposition of different inorganic and organic components (49,71). Pt and Au are the most widely used elements for fabricating photonic Vis-LDM (1). More recently, major updates in this technique have focused on using more economical metals or metal oxides that introduce new characteristics to Vis-LDM. The GLAD technique, associated with the E-beam technique, is a PVD variant where vapor is deposited at an adjustable angle, creating an elongated tail on one hemisphere of the Vis-LDM (72). The ED method use simultaneous oxidation and reduction to form solid coatings on substrates. It is more cost-effective than PVD and suitable for synthesizing Vis-LDM with controllable dimensions. Common techniques include membrane-assisted electrodeposition and bipolar electrochemical deposition, using alumina oxide and polycarbonate membranes. Recent improvements include deposition in controlled atmospheres and precise temperature conditions to minimize defects and improve film quality. Additionally, techniques for microscale deposition have been developed, enabling the fabrication of Vis-LDM with

View Article Online
DOI: 10.1039/D4VA00230J

specific characteristics in very small regions (44,69). Template-assisted electrochemical deposition provides precise control over morphology, enabling the formation of complex structures essential for optimizing photocatalytic efficiency and propulsion in Vis-LDM. It is scalable, straightforward, and allows for versatile material composition, incorporating dopants and modifiers tailored to specific applications. Operating efficiently with low energy consumption, this method ensures economic and environmentally friendly manufacturing, enhancing motor stability and performance.

Table 1 - Key findings concerning the photocatalyst materials and synthesis methods.

Conditions	Benefits	Limitations	Ways to overcome the limitations	References
Photocatalytic Materials Low bandgap photocatalysts				
gC_3N_4	High performance in aqueous media using low concentrations of H_2O_2	Rapid e^+/h^- recombination and inefficient charge separation	Structural modifications, doping, and heterojunction processes	(28–32)
Cu_2O	Facilitates the formation of heterojunctions and different morphologies	Limited photocatalytic efficiency and low chemical stability	Introduction of defects and control of crystal facets.	(34,35)
Ag_3PO_4	Increased effectiveness in generating reactive radicals	Photocorrosion and high cost	Doping, formation of composites, and incorporation into support matrices	(37–40)
BiOI	Efficient e^+/h^- separation and chemical stability	Low electrical conductivity and slow hole transfer	Morphological alternatives and formation of heterojunctions	(44–48)
Photocatalytic Materials High bandgap photocatalysts				
(TiO_2 and ZnO)	Chemical stability, low cost, non-Toxic and environmentally friendly	Limited visible light absorption and rapid charge recombination	Enhance visible light absorption: p-n junctions, surface doping, and dye sensitization.	(49–53)
Synthesis Methods Photocatalyst				
Sol-gel	Produces Vis-LDM with high surface area and controlled porosity	Complexity of process optimization and extended processing times	Use of the mildest synthesis conditions and explore faster drying and thermal treatment methods	(23)
Hydrothermal/ Solvothermal	Produces nanostructured	High processing temperatures and	Use reagents that allow for synthesis	(24)

View Article Online
DOI: 10.1039/D4VA00230J

	crystalline materials with tailored properties	pressures; Low reproducibility and homogeneity and potential for particle aggregation	at lower temperatures and employ stabilizing agents to prevent aggregation	
Electrochemical	Used for preparing Vis-LDM with tube forms; Simple, cost-effective, and scalable.	Difficulties in achieving precise and uniform control over the morphology of the produced structures	Adjust parameters such as current, voltage, and deposition time, and explore modifications in electrode conditions to achieve desired morphologies	(70)
Synthesis Methods Asymmetry required for movement				
Chemical Vapor Deposition (CVD) and Electrodeposition (ED)	CVD for depositing thin films and forming Janus structures. - ED for forming solid coatings with controlled dimensions.	Equipment cost and complexity, and difficult control of thickness and uniformity	Controlled atmospheres and temperature conditions.	(49,71)
Template-assisted Electrochemical Deposition	Provides control over morphology for optimized photocatalytic efficiency and propulsion.	Difficulty in removing templates and issues with uniformity and morphology control	Use templates that can be easily removed by physical or chemical methods, such as dissolution in appropriate solvents or thermal degradation	(44,69)

3. Vis-LDM photocatalysis applied to the degradation of environmental pollutants

Vis-LDM have been designed to enhance and accelerate the water decontamination process through the synergistic interaction between their active movement and their photocatalytic properties, allowing more efficient degradation of organic pollutants. The operation process of Vis-LDM involves two main stages: capture/adsorption and degradation. In the first stage, capture involves the physical adsorption or chemical binding of pollutants to the surface of the photocatalytic Vis-LDM (24). The efficiency of this adsorption is dependent on the surface characteristics of the Vis-LDM. Another significant point is that due to the micromixing and increased mass transfer in solution caused by the fast movement of Vis-

View Article Online
DOI: 10.1039/D4VA00230J

LDM, the degradation process is significantly enhanced (73). However, for the entire process to function efficiently, it is crucial to establish stable and robust contact between the Vis-LDM and the contaminants.

Ideally, these motors should also be programmed for selective adsorption of the contaminants of interest. However, such selective adsorption has not yet been described in the literature for Vis-LDM. Following the capture stage, degradation occurs, which is the core of water pollution treatment. This process involves chemical reactions that generate chemically active substances, primarily reactive oxygen species (ROS), to decompose pollutants into harmless substances such as H_2O and CO_2. This approach prevents secondary pollution, ensuring that no intermediate substances or new pollutants are formed (24). Photocatalytic Vis-LDM have been extensively studied for the photodegradation of different organic pollutants. Research has focused on a range of substances, such as pesticides (44,74) phenolic compounds (38,61,67,75) and phthalates. Additionally, there has been significant interest in the degradation of dyes (30,31,80–83,43–45,58,76–79), psychoactive drugs (73,84) and therapeutic agents (19,32,85–87). More recently, studies have explored the photodegration of explosives like picric acid, using tubular Vis-LDM based on $TiO_2/Fe_3O_4/CdS$ (88) as well as the degradation of microplastics components (29,46,89).

3.1 Benefits and Challenges of Using Photocatalytic Vis-LDM as an Emerging Technology for the Degradation of Environmental Pollutants

The use of photocatalytic Vis-LDM is revolutionizing environmental remediation by harnessing visible light energy for precise and efficient cleaning operations. These miniaturized devices integrate advanced engineering and materials science, enabling them to operate in complex and specific environments while minimizing harm to ecosystems (Figure 3). One of the most remarkable features of photocatalytic Vis-LDM is their ability to move in complex environments with precision. Due to their small size and high mobility, these robots can access and clean specific contaminated areas, minimizing collateral damage to surrounding ecosystems. This precision allows for a more targeted, efficient, and safe approach, especially in hard-to-reach locations (23).

Photocatalytic Vis-LDM reduce the need for harmful chemicals, offering an eco-friendly alternative for the degradation of environmental pollutants. While Vis-LDM most of the time they need H_2O_2, which is not inherently eco-friendly, they are comparatively more environmentally friendly than traditional methods for degrading environmental pollutants often involve substances that, while effective, can cause additional disruptions to ecosystems. Vis-LDM mitigate these adverse effects, providing a greener and less invasive alternative. Their versatility allows Vis-LDM to adapt to different tasks, such as cleaning oil spills and removing pollutants from water and air (3). Equipped with autonomous capabilities, these robots can operate continuously in remote or hazardous environments without the need for

View Article Online
DOI: 10.1039/D4VA00230J

constant human supervision, which is crucial in situations where human presence would be risky or impractical (24). Furthermore, their focus on energy efficiency and sustainability results in a reduced environmental footprint, making them ideal for long-term cleaning efforts. In summary, photocatalytic Vis-LDM have significant potential to effectively mitigate pollution, contributing to a cleaner and more sustainable future.

Figure 3. Schematic of the benefits and limitations highlighted until 2020, in the use of photocatalytic Vis-LDM in the degradation of environmental pollutants.

Despite the previously highlighted benefits, the practical application of photocatalytic Vis-LDM in the degradation of environmental pollutants faces significant challenges (Figure 3). Firstly, the materials used in the construction of Vis-LDM are subject to consumption through oxidation, resulting in a short useful life time (23). Research of new materials to prolong the durability of these devices is necessary. Enhancing the cost-effectiveness of Vis-LDM by increasing their useful lifetime and improving their stability and reusability is a crucial step. Furthermore, most photocatalytic Vis-LDM described up to 2020 rely on fuels such as H_2O_2, which is effective in pollutant degradation but generates reactive species like hydroxyl radicals (24). Fuel-free or biofuel-powered Vis-LDM should be explored as more sustainable alternatives (26). The cost of catalysts is also a challenge, as Pt and Au, commonly used, are expensive and toxic. The toxicity of materials is another concern since some can cause secondary pollution. Alternative materials that are economic, eco-friendly, and biocompatible need to be investigated (23). The removal of Vis-LDM after decontamination is an important challenge that needs to be addressed. Additionally, synthesis techniques need to be adapted for efficient and cost-effective industrial-scale production (2). Innovations in materials and synthesis methods are required to optimize Vis-LDM and overcome these challenges. The environment in which Vis-LDM operate also influences their performance.

A possible significant disadvantage of Vis-LDM is their limited navigation range, typically only a few millimeters. This limitation can impact their performance and applicability in pollutant treatment in several ways. Firstly, the reduced range implies that these motors can only operate effectively in very small areas, which limits their use in larger environments, such as large-scale wastewater treatment systems. Furthermore, the ability of the motors to distribute themselves uniformly across large areas is compromised, resulting in zones where the treatment is ineffective and pollutants are not adequately degraded. The distances travelled by LDM in general may be increased a few orders of magnitude if guiding steering systems are applied such as directed light sources or magnetic fields (90,91). However, such guiding systems may be of difficult practical implementation in the environment.

The gravitational sedimentation of Vis-LDM is another possible limitation that may significantly influence the performance of these devices in the environment. It is known that the shape and composition, density, propulsion mode, viscosity, among other factors, determine whether the LDM settle or not (92). If the conditions allow for settling and

View Article Online
DOI: 10.1039/D4VA00230J

stratification, their ability to move freely and reach all areas of the fluid is compromised. This results in decreased pollutant treatment efficiency. The accumulation of motors at the bottom can also obstruct flow channels, impacting system operation. For photocatalytic Vis-LDM, stratification can decrease light activation efficacy, as thicker layers at the bottom may prevent uniform light exposure, leading to irregular activation and reduced catalytic performance.

The composition of wastewater, including inorganic ions and sulfur, can affect the movement and efficiency of Vis-LDM, reducing their lifespan and effectiveness (3). To reach this innovation, the potential for collective work among these devices has been suggested to optimize their photocatalytic capacity. However, this is believed to be one of the parameters that will be studied later, due to other higher priorities and inherent difficulties (24).

Considering the main limitations identified in the use of photocatalytic Vis-LDM for the degradation of environmental pollutants, the following sections will present and discuss the innovations/modifications described in recent years to surpass them.

4. Most recent advances in photocatalytic Vis-LDM applied to the degradation of environmental pollutants

Recent advances found in the area of photocatalytic Vis-LDM were divided into three important points that respond to some of the main limitations mentioned previously.

4.1 More ecological, sustainable and biocompatible variants of Vis-LDM

As previously mentioned, most Vis-LDM depended on materials and processes that can be harmful to the environment, making them unsustainable in the long term. Additionally, many of these motors are not biocompatible, limiting their application in certain applications. In light of these challenges, there is the urge to develop eco-friendlier, sustainable, and biocompatible variants of Vis-LDM. The creation of motors that use biodegradable and non-toxic materials, sourced from the environment, along with manufacturing processes that minimize environmental impact, is crucial for advancing the large-scale use of these devices. Moreover, the development of new devices that use biofuels or even operate without the need for additional fuels, thereby enhancing movement and consequently increasing photonic activity, is essential. Therefore, the pursuit of greener and more environmentally friendly Vis-LDM is not only a matter of technological progress but also an ethical and environmental responsibility.

4.1.1 Absence of fuel or use of biofuels

The elimination of the need for fuel for the self-propulsion of Vis-LDM is a major concern, but it also presents significant challenges, as it is associated with a decrease in propulsion

View Article Online
DOI: 10.1039/D4VA00230J

speed and a consequent reduction in the photodegradative efficiency of these motors (49,78,84,93,94). The development of Vis-LDM that do not require conventional fuels for self-propulsion represents a recent advancement. These motors utilize exclusively visible light energy as a clean and abundant energy source to generate movement. However, the practical implementation of these Vis-LDM faces several technical challenges. One of the main difficulties is the efficiency of converting light energy into movement, which requires materials and mechanisms that can maximize this conversion efficiently and sustainably.

Rojas et al. (21) described the creation of Vis-LDM based on Ag_3PO_4 that self-propel efficiently without the need for external fuels. This was achieved by exploiting the different crystalline facets exposed on the surface of the micromotors. Using a scalable precipitation method, the researchers synthesized self-propelled Ag_3PO_4 particles in amorphous (am-Ag_3PO_4), cubic (c-Ag_3PO_4), and tetrahedral shapes (t-Ag_3PO_4) (Figure 4a). The t-Ag_3PO_4 demonstrated the highest movement capability due to their more active facets. In addition to movement capability, Ag_3PO_4 micromotors also exhibited fluorescence (Figure 4a), allowing their tracking by fluorescent methods. They showed antibiofilm activities against both gram-positive and gram-negative bacteria. The enhanced diffusion of the particles promoted effective biofilm removal, surpassing static methods (Figure 4b). This study investigated crystalline Ag_3PO_4 photocatalytic micromotors, as well as their static Vis-LDM analogs (in the absence of light), for eradicating bacterial biofilms of *Pseudomonas aeruginosa* (gram-negative) and methicillin-resistant *Staphylococcus aureus* (MRSA, gram-positive) using visible light, without the need for H_2O_2 during 7 days of incubation at 37 °C. Under static conditions, all micromotors reduced biofilm viability significantly: 66 % for am-Ag_3PO_4, 74 % for c-Ag_3PO_4, and 45 % for t-Ag_3PO_4. When the micromotors were in motion, viability dropped further to 17 % for am-Ag_3PO_4, 57 % for c-Ag_3PO_4, and 15 % for t-Ag_3PO_4. These micromotors also notably decreased biofilm thickness for *P. aeruginosa* from 77 μm in control samples to 45 %, 38 %, and 18 % of the original thickness for am-Ag_3PO_4, c-Ag_3PO_4, and t-Ag_3PO_4, respectively. For MRSA, the micromotors were even more effective, with viability reduced to 1 % for am-Ag_3PO_4, 32 % for c-Ag_3PO_4, and 18% for t-Ag_3PO_4 under static conditions, and further to 0.5 %, 4 %, and 4 % under moving conditions. Biofilm thickness also decreased significantly from 19 μm in the control to 9 μm for am-Ag_3PO_4, 8 μm for c-Ag_3PO_4, and 13 μm for t-Ag_3PO_4. The different efficiencies between MRSA and *P. aeruginosa* are attributed to variations in biofilm matrix composition and the autoaggregation capabilities of the pathogens, with *P. aeruginosa* showing greater biofilm complexity. This work suggests a Vis-LDM for biofilm eradication, without the need for H_2O_2, more efficient against MRSA biofilms than *Pseudomonas aeruginosa*.

Figure 4. a) Fluorescence microscopy images of Vis-LDM based on Ag_3PO_4 in tetrahedral, cubic, and amorphous forms in pure water under light excitation (λ = 488 nm); b) Effect of

View Article Online
DOI: 10.1039/D4VA00230J

Vis-LDM on *methicillin-resistant S.* aureus biofilms under visible light irradiation and in the dark for 60 minutes. C (control): without light irradiation and Vis-LDM, S (static): in the presence of Vis-LDM and M (moving): in the presence of Vis-LDM and light. Adapted from (21) (Licensed under an open-access Creative Commons CC BY 4.0 license).

A recent study described an easy and scalable method to produce hybrid inorganic-organic tubular Vis-LDM, consisting of a mesoporous silica structure coated with an organic semiconducting triazine-thiophene polymer (Tz-Th) (84). These Vis-LDM were applied in the capture and degradation of psychoactive drugs in wastewater effluents, particularly methamphetamine derivatives. The synthesis process involved a mesoporous silica template combined with an active polymer containing thiophene and triazine units. The well-defined tubular structure of these motors allowed for efficient directional movement under visible light without the need for fuel, also exhibiting lifting and rotational movements due to the polymeric coating accumulation. Under visible light irradiation, these Vis-LDM could degradation methamphetamines into smaller organic fragments within 20 minutes, achieving complete removal of intermediates after 2 hours. Two aspects stand out in this work: firstly, the targeted photocatalytic degradation of hard to degrade and highly hazardous pollutants in water effluents, by the exclusive effect of light without the need for other fuels, that offering an innovative and practical solution to environmental problems related to drug contamination; secondly, the low-cost and scalable synthesis process using easily available precursors, and the well-defined morphology that provides stability and efficient propulsion in aqueous media.

The complexity of the mechanisms required for self-propulsion without traditional fuels increases the difficulty in constructing these motors. Vis-LDM need sophisticated systems that can capture and utilize light effectively, transforming it into continuous movement without the need for external interventions or refueling. This may justify the limited investment in recent years in this emerging challenge in the field of photocatalytic Vis-LDM. The use of biofuels for the self-propulsion of Vis-LDM has been explored, as a viable alternative to overcome the limitations of not using fuels (13,75,88). Biofuels are generally less polluting and can be used in many existing motors with some modification, facilitating the transition to more sustainable energy sources. Additionally, they ensure the energy conversion efficiency of Vis-LDM due to their specific chemical and physical properties, maintaining self-propulsion and consequently photocatalytic efficiency, which is often compromised in the absence of fuel.

Yang et al. (13) developed a highly efficient Vis-LDM based on Cu_2O@GO, capable of utilizing different biocompatible fuels. Due to doping with graphene oxide (GO), these micromotors exhibit enhanced photocatalytic performance and can be activated by both visible light and near-infrared (NIR) light. GO contributes to better charge separation, increased surface area, enhanced light absorption, and the introduction of local photothermal

View Article Online
DOI: 10.1039/D4VA00230J

effects. These improvements enable the Vis-LDM based on Cu_2O@GO to be efficiently propelled by biocompatible fuels and sustainable energy. Compared to conventional Cu_2O micromotors, which operate only under visible light, Cu_2O@GO micromotors demonstrated speeds three times faster under full visible light with glucose fuel. Furthermore, due to the enhanced photocatalytic and local thermal effects provided by GO, these micromotors demonstrated propulsion under NIR using biocompatible fuels such as glucose, leucine, and urea, achieving speeds of up to 11.5 µm/s with glucose. This new approach of GO doping significantly improves the propulsion of traditional LDM, extending their activation to include NIR light, and enabling efficient propulsion using biofuels.

In another study, Kutorglo et al. (75) demonstrated the possibility of using photoactive and enzymatic systems for developing Vis-LDM with proven photocatalytic activity in the removal of organic pollutants. Using a scalable synthesis process, light-absorbing polypyrrole nanoparticles were impregnated in a bienzymatic system composed of glucose oxidase (GOx) and catalase (Cat). This design enabled the creation of Vis-LDM that efficiently degrade organic pollutants using only visible light and a biofuel, glucose. The impregnation to the enzymatic system allowed the simultaneous use of light and glucose as energy sources. GOx uses glucose to produce H_2O_2, which is then decomposed by Cat, generating active radicals and oxygen bubbles that propel the nanoparticles. Visible light heats the nanoparticles, activating enzymatic activity. The irregular distribution of GOx and Cat on the nanoparticle surface results in non-homogeneous peroxide creation and degradation, providing random propulsion to the Vis-LDM. These new nanomotors were tested in the degradation of chlorophenol, demonstrating a removal capacity exceeding 95 % of chlorophenol in 1 hour, without the need for external agitation, in the presence of glucose (5 % *v/v*).

The use of biofuels for the self-propulsion of Vis-LDM faces several significant challenges. One of the main difficulties is the need to continuously supply a source of biofuel, which can be logistically complex and economically impracticable on a large scale. Additionally, there is a possibility of deterioration of biofuels over time, which can compromise the efficiency and durability of Vis-LDM. Moreover, the integration of biofuels with micromotors requires fuel storage and delivery systems, increasing the complexity and cost of the design and manufacture of these devices. Despite being a good option, the absence of the need for fuels will always be the best option.

4.1.2 Use of natural resources for Vis-LDM production

The use of biological resources for the production of Vis-LDM presents several advantages, including the sustainability and reusability, biocompatibility, and the ability to integrate enzymes and biomolecules to create innovative and efficient propulsion mechanisms (81,87,93,95–97).

View Article Online
DOI: 10.1039/D4VA00230J

Recently, the utilization of biological resources to produce Vis-LDM gained an increased importance. A notable example is the use of lignin, an abundant and sustainable biological resource, ideal for producing carbon-based functional materials due to its high carbon content (~60 %) and different phenolic units. A recent study employed lignin for photocatalytic and self-propulsion applications (81). Initially, precursor carbon particles rich in hydroxyl groups, called HCLSs, were prepared through the hydrothermal carbonization of lignin microcapsules (Figure 5a). Upon heating these urea-coated HCLSs, carbon spheres with a gC_3N_4 layer were formed, providing the essential -OH groups for the formation of photocatalysts (Figure 5b). After coating one side of the spheres with Pt/Pd, they became self-propelling in the presence of fuel such as H_2O_2 and under visible light irradiation. These new photocatalytic Vis-LDM demonstrated enhanced activity, degrading 49 % of the pollutant RhB in 60 minutes at an intensity of 100 mW/cm². The removal rate was three times higher compared to Vis-LDM based on gC_3N_4.

Figure 5. (a) Synthesis scheme of g-C_3N_4@CSs from Kraft lignin and urea. (b) Proposed molecular interactions between urea and the surfaces of CSs (made of acetylated lignin) and urea/HCLSs, with and without the presence of -OH groups on the surfaces of HCLSs. Adapted from (81) (Licensed under an open-access Creative Commons CC BY 4.0 license).

Dhar et al. (82) described the creation of Vis-LDM inspired by biological motors, utilizing modified cellulose nanocrystals (CNCs) for self-propulsion. These nanomotors were capable of degrading pollutants and performing magnetic hyperthermia to clear arterial plaques. Derived from renewable biomass, the CNCs were decorated with catalytically active and magneto-responsive nanoparticles (Fe_2O_3/Pd) in a sustainable means. These Vis-LDM exhibited enhanced propulsion with lower concentrations of H_2O_2, remotely controlled by chemomagnetic field gradients. The motion associated with these Vis-LDM was propelled by heterogeneous bubble dynamics, degrading pollutants and generating heat through hyperthermia, increasing degradation rates in real-time. In a microfluidic channel, their dynamics were controlled by magnetic fields and pH gradients, representing chemotaxis in cell-like environments. For the evaluation of the photocatalytic performance of Vis-LDM based on CNC in pollutant degradation, methylene blue (MB) was used as the model pollutant. The nanomotors modified with Fe_2O_3 and Pd nanoparticles showed a significantly improved degradation rate compared to unmodified CNCs. The FeCNC nanomotors exhibited a degradation rate (k_{FeCNC}) of 0.470 mg/L/min, while the Pd-FeCNC nanomotors achieved a $k_{Pd-FeCNC}$ of 1.04 mg/L/min, attributed to the generation of peroxide radicals by Fe^{2+} ions and the catalytic activity of Pd nanoparticles. These Vis-LDM did not require toxic fuels and were able to degrade the dye within 10 minutes at low concentrations. The adsorption of MB was enhanced by the hydrophilic nature and negative surface charge of the CNCs. However, the catalytic activity decreased over time due to the poisoning of the nanomotors, caused by the release of iron or palladium ions, which altered the motion dynamics of the Vis-LDM.

View Article Online
DOI: 10.1039/D4VA00230J

In another study, tubular Vis-LDM nanorockets based on halloysite with self-propulsion controlled by chemicals and visible light were developed (87). Halloysite is a natural clay mineral with a unique tubular structure, known as halloysite nanotubes (HNTs). This mineral has been explored in environmental remediation and catalysis, but only with this work has its application for Vis-LDM preparation been demonstrated (94). Compared to traditional manufacturing of tubular micro/nanomotors, this approach has the advantage of using natural clay as a substrate, which is abundant and does not require complex equipment. In this study, HNT nanorockets were further modified with silver (Ag) and α-Fe_2O_3 nanoparticles to achieve greater photodegradation performance compared to control samples using only a self-propulsion mechanism. This improvement in propulsion speed results from efficient charge separation within the α-Fe_2O_3 photocatalytic layer. Electrons from the valence band of Fe_2O_3 migrated to the conduction band and became trapped in the metallic layers of the Ag particles, resulting in a net negative charge on the Ag particles. These electrons on the surface of Ag facilitated the decomposition of H_2O_2, generating more bubbles and consequently better propulsion (Figure 6).

Figure 6. Band structure of the Ag–Fe_2O_3 heterostructure and schematic illustration of a visible light-enhanced propulsion mechanism. Reprinted with permission from (87) (Copyright © 2022 American Chemical Society).

To assess the photocatalytic performance of Vis-LDM nanorockets for water remediation, tetracycline hydrochloride was used as a model contaminant. The three-component Ag−Fe_2O_3/HNTs nanorockets achieved a 91 % removal efficiency within 30 minutes under visible light, outperforming α-Fe_2O_3/HNTs (61 %) and Ag/HNTs (57 %). The removal efficiency was significantly reduced without H_2O_2, highlighting its importance. Kinetic analysis showed the highest rate constant (0.045 min^{-1}) for Ag−Fe_2O_3/HNTs. The nanorockets exhibited high stability over multiple uses. Radical scavenging tests indicated that •OH was the dominant species in the degradation process, as other radicals had minimal impact. The photocatalytic performance of various catalysts was evaluated using electron paramagnetic resonance (EPR) to measure hydroxyl radicals (•OH) and confirm degradation mechanisms. The spin-trapping agent DMPO was used, revealing that Ag−Fe_2O_3/HNTs generated more •OH than Ag/HNTs or α-Fe_2O_3/HNTs, which aligned with its superior degradation performance.

A similar study was described by Xing et al. (96) where Vis-LDM based on NiMn-CLDH nanosheets functionalized with ascorbic acid (AA-NiMn-CLDHs@HNTs-Ag) were discussed. These nanomotors were assembled from NiMn-CLDH nanosheets with intrinsic oxidase/peroxidase activity and HNTs, forming a unique 3D hierarchical architecture with more accessible reactive sites. Silver nanoparticles were introduced into the HNTs lumen, acting as catalysts for H_2O_2 decomposition to produce O_2 bubbles for nanomotor propulsion. Benefiting from autonomous motion, 3D hierarchical morphology, and robust peroxidase-

View Article Online
DOI: 10.1039/D4VA00230J

like activity, AA-NiMn-CLDHs@HNTs achieved enhanced photocatalytic activity for phenol degradation (89 % in 30 minutes, by Fenton reaction).

Recently, new Vis-LDM based on galactooligosaccharides were designed for visible-light-controlled water disinfection, addressing the serious hazard posed by waterborne pathogens to potable water sources (97). These Vis-LDM are recognized as promising agents for *in vivo* antibacterial therapy, yet face significant challenges in water disinfection. The study described the use of galactooligosaccharide-derived N-nitrosamines as visible light-sensitive fuel for spontaneous antibacterial nitric oxide production by nanomotors. This solar-to-chemical energy conversion powered nanomotor self-diffusiophoresis, enhancing diffusion in water and biofilm penetration, leading to significant pathogen and biofilm inhibition and elimination in aquatic environments. Post-treatment, prebiotic-based disinfectant residues can be selectively utilized by beneficial bacteria, effectively reducing environmental and human health risks. To assess the water disinfection capabilities of prebiotic nanomotors, an aqueous suspension of preformed biofilms (1 cm × 1 cm) was treated with 600 μg of these nanomotors under sunlight. Unlike the control biofilms, which showed no significant change, the biofilms treated with Vis-LDM were almost completely dissociated after 5 hours of irradiation. This treatment resulted in a dramatic reduction in colony-forming units (CFU) from 3.33×10^7 CFU/mL in the control to approximately 500 CFU/mL, achieving a bactericidal rate of 99.99 %. These antibacterial Vis-LDM were efficient, eco-friendly, and low-energy, showing promising potential for water disinfection.

Moreover, Xue et al. (95) presented a novel biocatalytic Vis-LDM based on a covalent organic framework (COF), intelligently controlled by visible light due to the presence of a photosensor and catalase. This Vis-LDM comprised a mesoporous COF (RT-COF-1) as a matrix for loaded spiropyran (PAH), a molecular photosensor that changes spatial conformation upon exposure to specific wavelengths of light, enabling light-controlled substituting of the nanomotor mechanism. Additionally, encapsulated catalase (CAT) within the COF established an H_2O_2 concentration gradient between the nanomotor surface and the surrounding solution, resulting in self-propelled motion. These Vis-LDM demonstrated efficiency in RhB removal through self-diffusiophoresis and enhanced Brownian motion. The Vis-LDM speed was precisely adjusted by alternating between different wavelengths of light due to the photoisomerization of the incorporated photo-switch. Under blue light, the nanomotor exhibited high efficiency in RhB removal, achieving 79.8 % removal in just 30 minutes, significantly reducing adsorption time and energy consumption without manual stirring (Figure 7a). When using the red light, the Vis-LDM motion and contaminant removal were deactivated. Furthermore, the nanomotor allowed for on-demand RhB removal by simply switching between blue and red light, contributing with an innovative approach for light-controlled water remediation) (Figure 7b).

View Article Online
DOI: 10.1039/D4VA00230J

Figure 7. Results of: a) removal of RhB over time by Vis-LDM under blue, red and dark irradiation in a solution containing 50 mM H_2O_2; b) removal of RhB by Vis-LDM under red/blue light switch (5 minutes each, red line) and when kept in the dark (black line). Reprinted with permission from (95) (Copyright © 2023 American Chemical Society).

Despite these advancements, the integration of biological components with inorganic or synthetic materials requires precise control of manufacturing conditions to ensure compatibility and performance. Furthermore, the variability of biological resources, the stability and durability of biocomponents, and the need for efficient synthesis and purification techniques for large-scale production pose significant challenges. Nevertheless, this is a rapidly expanding field crucial for the development and prosperity of Vis-LDM photocatalysts applied to environmental pollutant removal.

4.2 Enhancing Self-Propulsion and Subsequent Photonic Activity

4.2.1 Combination of Visible Light with Other External Parameters

The strategic combination of visible light with other external parameters can lead to significant advancements in the efficiency and functionality of Vis-LDM. By carefully adjusting the light intensity and wavelength, as well as the chemical and physical environment, it is possible to optimize self-propulsion and photonic activity, making way for increased interest in these devices optimized for the photodegradation of environmental pollutants. The combination with magnetic fields is the most studied strategy in recent years, allowing the guidance and/or control of Vis-LDM direction (31,49,74,83,86,88,89,98).
In one study, hybrid-powered Vis-LDM were prepared, based on photocatalytic ($BiVO_4$) and magnetic (Fe_3O_4) materials, designed to self-propel under sunlight and operate precisely under a magnetic field within macrochannels (89). These motors demonstrated an efficient capacity to degrade different synthetic microplastics. The $BiVO_4$-based photocatalytic motors were shown to efficiently self-propel in aqueous media under visible light, attaching to microplastics with different polymer structures, including polylactic acid (PLA), polycaprolactone (PCL), polyethylene terephthalate (PET), and polypropylene (PP), subsequently degrading them into small organic molecules and oligomers (Figure 8). The combination of visible light irradiation and a magnetic field enabled controlled movement within multichannels, accelerating the photodegradation process. For the first time, Vis-LDM demonstrated the capability to capture and transport a large amount of microplastics in a complex labyrinth in response to sunlight, in addition to efficiently degrading them into smaller oligomers and polymers. The study investigated the photocatalytic degradation of plastics using various methods. Microplastics were treated with photocatalysts under visible light, showing gradual weight loss over 7 days. PLA experienced the most degradation (~70 %), while PCL, PET, and PP were less affected (~10 %), Plastics treated with photocatalysts showed increased hydrophilicity and surface roughness. X-ray photoelectron spectroscopy

View Article Online
DOI: 10.1039/D4VA00230J

and scanning electron microscopy confirmed oxidation and morphological changes. The photocatalysts effectiveness declined after 7 days, but they could be recovered due to their magnetic properties. This method was energy-efficient, driven solely by wireless energy, without the need for pre-treatment or bulky mechanical agitators used in conventional systems, offering an alternative approach for the real-time removal and degradation of different microplastics.

Figure 8. Representative scheme of the autonomous movement, capture, transport and degradation of microplastics by Vis-LDM based on $BiVO_4/Fe_3O_4$ under a solar simulator in a labyrinth with five channels, with lengths of 0.4 cm (ii), 0.6 cm (iii) and 0.8 cm (iv), in the presence of H_2O_2 0.1 % *v/v*. Reprinted with permission from (89) (Copyright © 2021 American Chemical Society).

Zheng et al. (31) described heterogeneous Vis-LDM fabricated by a one-step hydrothermal method that simultaneously deposits gC_3N_4 photocatalysts and Fe_3O_4 magnetic nanoparticles onto kapok fibers (KF), creating gC_3N_4-Fe_3O_4@KF micromotors. These devices, remotely controllable by visible light, exhibited linear movement and self-rotation in the presence of H_2O_2, with speed modulated by the concentration of H_2O_2 and light intensity. The addition of Fe_3O_4 nanoparticles enhanced the photocatalytic Fenton reaction, increasing the production of reactive species for the degradation of environmental pollutants. The study demonstrated that the combination of photocatalytic Fenton oxidation with enhanced mass transfer due to self-propulsion and self-rotation resulted in significantly more efficient degradation of RhB dye (99.8 % in 60 minutes) compared to stationary systems. The magnetic properties of the Vis-LDM facilitated their collection and recycling.

Building on previous work, dual-mode Vis-LDM based on foam-like carbon nitride (fC_3N_4) with Fe_3O_4 nanoparticles (Fe_3O_4/fC_3N_4) demonstrated self-propulsion through chemical and magnetic stimuli, which increased photocatalytic activity and subsequent degradation of organic pollutants (86). These Vis-LDM exhibited a three-dimensional porous structure, attributed to the presence of fC_3N_4, and efficient photocatalytic performance under visible light with low H_2O_2 levels (≤2 %) due to the presence of Fe_3O_4 nanoparticles (~50 nm). The The Vis-LDM, when exposed to visible light, initially showed modest tetracycline removal efficiency, improving from 10 % to 40 % as light intensity increased (300 and 600 mW cm^{-2}), in 80 min. However, with the addition of H_2O_2, efficiency significantly increased, reaching up to 96.4 % with 2 % H_2O_2. The enhanced photoactivity was due to electron trapping by Fe_3O_4 nanoparticles, resulting in greater visible light absorption and efficient e^+/h^- pair separation. Under an external magnetic field, the collective behavior of the Vis-LDM significantly increased the local concentration of catalysts, improving pollutant removal efficiency. The magnetic properties of Fe_3O_4 facilitated recycling and enabled targeted catalysis.

View Article Online
DOI: 10.1039/D4VA00230J

Shivalkar et al. (74) presented adaptable Vis-LDM effective in adverse environmental conditions, taking advantage of the improved movement associated with external magnetic fields and medium temperature. These micromotors, composed of carbon dots, iron oxide nanoparticles, and a thermosensitive polymer (Pluronic-F127), were capable of moving at long distances in hostile environments, making them viable for water treatment. These Vis-LDM demonstrated programmable and controllable propulsion in response to stimuli such as pH, temperature, and viscosity, exhibiting low cytotoxicity and being fabricated from economical precursors. The cylindrical thermosensitive magnetic Vis-LDM exhibited controlled movement using magnetic fields and temperature, demonstrating functional efficacy and adaptability for complex operations. The thermosensitive polymer allowed the micromotors to be monitored, reused after magnetic separation, or self-destructed depending on the medium temperature. They were effective in degrading toxic pesticides like profenofos, achieving over 70 % degradation in about 8 hours under standard conditions (pH = 4.5 and viscosity of 1 %). Even in more viscous medium (pH = 8.5 and viscosity of 5 %), the degradation rate was 60 % in 8 hours, showing efficiency in pollutant removal.

4.2.2 Enhancing Visible Light Absorption Capacity

Enhancing the visible light absorption capacity of Vis-LDM is crucial to improve their self-propulsion and photonic activity. This results in higher energy efficiency, improved propulsion, greater versatility, and sustainability, making these devices more effective and applicable in different technological and environmental areas. Numerous studies have focused on enhancing light absorption capacity to improve the performance of photocatalytic Vis-LDM. The primary strategies adopted include modifications to activate Vis-LDM, specifically doping (29,79,85,99), heterojunction formation (30,44,76) and crystallinity adjustments (21,36,80,100).

Doping

Self-propelled spherical bubble-driven Vis-LDM (Pt-$ZnIn_2S_4$) with high mobility and photocatalytic performance, designed for photocatalytic water purification, were described by Yuan et al. (99). Using a simple and efficient UV reduction method, Pt doping in $ZnIn_2S_4$ microspheres formed by nanosheets was demonstrated. The Pt nanoparticles enhanced the separation and migration of photogenerated carriers at the semiconductor interfaces, improving visible light absorption due to their electron-accepting capability as cocatalysts and the localized surface plasmon resonance effect. The asymmetric structure of Pt-$ZnIn_2S_4$ micromotors facilitated the decomposition of H_2O_2, generating oxygen bubbles that propelled the Vis-LDM at a maximum speed of 970 ± 150 μm/s. Compared to traditional photocatalysts, the bubble-collapse-driven movement of the new Pt-$ZnIn_2S_4$ micromotors

View Article Online
DOI: 10.1039/D4VA00230J

improved solution agitation and mass transfer, allowing more efficient and rapid degradation of methyl orange (MO) dye and tetracycline hydrochloride (TCH) without the need for mechanical stirring.

In another study, a chemical precipitation method was used to synthesize Fe-doped ZnO-CdS-based Vis-LDM with enhanced visible light absorption (79). The new Fe-doped Vis-LDM exhibited strong room-temperature ferromagnetism and approximately 7 % improved photocatalytic efficiency compared to undoped ZnO-CdS nanocomposites. The photocatalytic performance of Fe-doped ZnO-CdS Vis-LDM was evaluated for the degradation of MB dye under visible light. The study compared Fe-doped ZnO-CdS with pure ZnO and ZnO-CdS nanocomposites. The energy band theory suggests that heterostructured nanocomposites, like ZnO-CdS, have altered bandgaps due to the interactions between different materials, which can enhance photocatalytic activity. Among the tested catalysts, Fe-doped ZnO-CdS demonstrated superior performance. Pure ZnO achieved a 31 % degradation of MB dye, while ZnO-CdS improved this to 71 % in 80 minutes. The Fe-doped ZnO-CdS nanocomposite outperformed both, achieving a 78 % degradation, in the same conditions. This enhancement was attributed to the increased visible light absorption capacity imparted by the Fe doping, which significantly boosted the inherent light absorption capabilities of the micromotors.

Liu et al. (85) described the synthesis of Vis-LDM based on Au-doped ZnO, using vertically aligned ZnO arrays, for enhanced photocatalytic degradation of tetracycline. Due to efficient movement capacity and charge separation improved by the vertical alignment of ZnO array combined with Au doping, these light-driven nanomotors removed approximately all tetracycline (40 mg/L) in 30 minutes and maintained stable photocatalytic activity for four cycles without apparent deactivation. The enhanced photocatalytic performance of Au-doped ZnO nanomotors with vertically aligned ZnO arrays is attributed to several factors. The vertical alignment facilitates efficient charge carrier movement and reduces electron-hole recombination. Au doping enhances charge separation by capturing electrons and promotes photocatalytic efficiency through surface plasmon resonance (SPR), increasing light absorption. This structure provides a large surface area and more active sites for the reaction, maintaining stability and preventing Au leaching over multiple cycles. The system generates reactive oxygen species (ROS) under visible light, effectively degrading tetracycline into non-toxic byproducts. This results in a highly efficient, stable photocatalytic system for environmental applications. This strategy developed to enhance antibiotic degradation shows great potential for environmental management.

Heterojunction formation

Spherical Vis-LDM based on carbon microspheres (CMS) coated with gC_3N_4 demonstrated enhanced capability for photodegradation of organic pollutants (30). The morphology and

View Article Online
DOI: 10.1039/D4VA00230J

composition of the gC_3N_4@CMS micromotor were identified as the main factors responsible for the higher photonic capacity acquired, as a result of the increased absorption capacity of visible light. Asymmetric photocatalytic redox reactions at gC_3N_4 on the symmetrical surface of the carbon micromotor under visible light improved bubble propulsion. This occurred because gC_3N_4 forms a highly catalytic microporous structure, facilitating bubble evolution in addition to increasing the surface area available for light absorption. Thus, self-propulsion reached speeds exceeding 168 μm/s under visible light with power of 250 mW/cm² in the presence of 30 % H_2O_2 (Figure 9). The high photocatalytic activity of porous gC_3N_4, combined with the rapid movement of Vis-LDM, resulted in accelerated degradation of RhB in 60 minutes under visible light (96 %), a performance twice superior to micromotors without propulsion. In addition to their high performance, these gC_3N_4@CMS micromotors present the advantage of low cost and simple structure, facilitating large-scale manufacturing.

Figure 9. Schematic representation of: (a) the self-propulsion by g-C_3N_4@CMS micromotors; (b) speed of g-C_3N_4@CMS micromotor *versus* H_2O_2 concentration; (c) speed of g-C_3N_4@CMS micromotor *versus* light intensity. Adapted from (30) (Licensed under an open-access Creative Commons CC BY 4.0 license).

Zhou et al. (44) developed Vis-LDM based on rGO/ZnO/BiOI/Co-Pi/Pt in such a way that ZnO nanoparticles increased the electronic mobility of the motor for electron transfer, the transparent conductive films of reduced graphene oxide rGO acted as electron acceptors, while cobalt phosphate (Co-Pi) accepted holes, thus enhancing BiOI with catalytic sites to improve light absorption, charge separation, and consequently more efficient surface reactions. Pt nanoparticles were crucial in catalyzing the degradation of H_2O_2, generating bubbles to drive the tubular Vis-LDM. RhB degradation tests revealed that Vis-LDM based on BiOI degraded 94 % of dye molecules in 30 minutes under visible light, compared to only 5.2 % in the dark. The combination of real-time chemistry, collective behavior of micromotors, and visible light-excited BiOI photocatalyst action provided an efficient and active platform for water purification.

The combination of heterojunction strategies involving two photocatalysts along with doping has also been explored and has proven to be a highly promising option. For example, Dharmana et al. (76) described Vis-LDMs based on ZnO/SnS core-shell heterojunctions doped with V_2O_5 for enhanced photocatalytic activity in the removal of MB under 300 W visible light illumination. In this work, the heterojunction was crucial for creating mixed crystalline phases on the Vis-LDM surface, leading to a plasmonic effect. Coupled with V_2O_5 doping, which adjusted the semiconductors bandgap, this resulted in improved visible light absorption, enhancing both the motors self-propulsion and the speed and efficiency of pollutant removal, achieving degradation rates of over 96 % in 2 hours.

View Article Online
DOI: 10.1039/D4VA00230J

In another study, Dai et al. (29) described plasmonic $Ag/Ag_3PO_4/gC_3N_4$-based Vis-LDM, where the gC_3N_4 nanosheet was uniformly wrapped around the Ag_3PO_4 nanopolyhedron, resulting in a hybrid nanomotor. A charge transfer bridge formed between Ag_3PO_4 and gC_3N_4 due to the reduction of Ag nanoparticles, inhibiting e^+/h^- pair recombination and promoting the transfer of photogenerated carriers to produce more active species in the photocatalytic reaction (Figure 10). The surface plasmon resonance of Ag nanoparticles improved visible light absorption and utilization. This hybridization, compared to Ag_3PO_4 and Ag/Ag_3PO_4 motors, exhibited higher photocatalytic activity, with a phenanthrene degradation rate of 0.01756 min^{-1}, being three times and twice higher than Ag_3PO_4 and Ag/Ag_3PO_4, respectively. Additionally, it was observed that after four reaction cycles, the $Ag/Ag_3PO_4/gC_3N_4$ photocatalyst maintained high photocatalytic activity, likely due to Ag doping, which increased the chemical resistance of Vis-LDM by inhibiting photocorrosion.

Figure 10. Schematic representation of Vis-LDM based on $Ag/Ag_3PO_4/gC_3N_4$ with representation charge transfer in a heterostructure. Reprinted with permission from (29) (Copyright © 2022 WILEY-VCH).

Crystallinity adjustments

The crystallinity of a material significantly influences its light absorption capacity through its ordered structure, photon absorption efficiency, and enhanced electronic properties. All these influence the propulsion and photocatalytic performance of Vis-LDM. Zhu et la., described that growth of Cu_2O crystal facets can significantly impact its optical and electrical properties, with {110} and {111} facets exhibiting high activity (80). The excellent crystallinity of Cu_2O can inhibit the recombination of photo-generated charges, improving its photocatalytic activity. However, photocatalytic Vis-LDM based on Cu_2O typically exhibit a spherical shape, resulting in low crystallinity and limited exposure of crystal facets, leading to weak separation of photoexcited e^+/h^- pairs and light-driven propulsion. Therefore, current research focuses on adapting crystal morphology and preserving facets with controllable indices in a single colloid. In another study polyhedral architectures of Cu_2O with well-defined facets (including low-index facets of {100}, {111}, and {110}, and high-index facets of {211}, {311}, {332}, and {544}) have been described to enhance photocatalytic properties and effective separation of photo-generated e^+/h^- pairs (36). Truncated octahedral Cu_2O nanomotors exhibited stable performance and vigorous movement under visible light, even at high temperatures (70 ºC), due to the efficiency of separation of photo-generated e^+/h^- pairs, demonstrating efficacy in various irradiations conditions (blue and green light) and with different types of biofuels, (pure water, glucose, and tannic acid). Compared to a spheroid, a polyhedral crystal of Cu_2O with higher crystallinity and more exposed controllable index facets exhibited more vigorous movement under visible light due to faster and better separation efficiency of photo-generated e^+/h^-

View Article Online
DOI: 10.1039/D4VA00230J

pairs, due to the formation of a heterojunction surface between {100} and {111} facets (Figure 11).

Figure 11. a) Scheme of the propulsion mechanism of a truncated octahedral Vis-LDM based on Cu_2O in pure water under visible light irradiation. (b and c) Motion trajectories of spherical (b) and truncated octahedral (c) Cu_2O motors over 3 seconds. Scale bar: 5 mm. Reprinted with permission from (36) (Copyright © 2021 Royal Society of Chemistry).

The photocatalytic performance of Cu_2O and TiO_2 nanocomposites was evaluated for MB dye degradation. Among the tested materials, the truncated octahedral Vis-LDM based on Cu_2O demonstrated the best performance, reducing the total MB degradation time from 80 to 50 minutes compared to pure Cu_2O nanoparticles. The photocatalytic efficiency increased with the amount of Vis-LDM nanowires and octahedrons achieved MB degradation in 35 minutes, faster than other forms. This improvement is attributed to the enhanced separation of e^+/h^- pairs provided by the p-n heterojunction between Cu_2O and TiO_2. Results show that truncated octahedral Vis-LDM based on Cu_2O exhibit nearly double the photocatalytic efficiency compared to pure Cu_2O, mainly due to the anatase structure and exposed {111} facets that facilitate charge transfer and enhance dye degradation.

Studying different crystallinity phases, including the amorphous phase, of Vis-LDM based on Ag_3PO_4 and with two distinct morphologies, cubic and tetrahedral, allowed the identification of distinct and more adjustable self-propulsion forms under different working conditions, namely without fuel or surfactants (21). The enhanced movement of the particles promoted biofilm removal in comparison with static control experiments, demonstrating the possibility of a new class of light-driven biofilm-eradicating micromotors that do not require the use of both H_2O_2 and UV light. Differences in these movement were detected according to morphology, which were correlated with photocatalytic activity. It was the tetrahedral Vis-LDM based on Ag_3PO_4 with dominant {111} facets exposed on the surface that showed more efficient propulsion movement and consequently higher biofilm inactivation activity. These results make sense considering that the dominant facets in this morphology were the most photonically active, allowing for more efficient bacterial biofilm inactivation by visible light photodegradation as abovementioned (section 4.1.1).

4.3 Enhancing Stability, Reusability and Collective Behavior

Enhancing the stability and reusability of Vis-LDM is crucial for several reasons. Firstly, it prolongs the useful life time of the devices, ensuring consistent and durable operation over time. Furthermore, it contributes to improved efficiency and more consistent photonic activity. Economically, the efficient reusability of Vis-LDM reduces costs associated with maintenance and manufacturing, in addition to conserving resources. In terms of applicability, more stable and reusable motors can be used in a variety of conditions and

View Article Online
DOI: 10.1039/D4VA00230J

experiments, making them more flexible and versatile. Environmentally, the reuse of Vis-LDM reduces waste generation and the environmental impact associated with the production and disposal of new devices. Recently, there has been concern about demonstrating the stability, but mainly the reusability of Vis-LDM (42,45,77).

In the study by Zhan et al. (42) the focus was on preparing photocatalytic Vis-LDM that could be easily recovered and reused in the degradation of organic pollutants. Using a simple hydrothermal method (Figure 12), BiOI/AgI/Fe_3O_4/Au micromotors were produced. The BiOI/AgI heterojunction it was responsible for increased stability of the photocatalytic Vis-LDM due to reduced charge recombination, improved charge separation efficiency, better adsorption of reagent molecules, and prevention of corrosion and degradation caused by visible light activity. Additionally, the integration of Fe_3O_4 allowed for the recyclability and reusability of the Vis-LDM, confirmed by the application of a magnet. After four reuse cycles, one hour each, a slight reduction in the RhB degradation rate was observed, from 53.2 % to 44.3 %, demonstrating the viability of recovering and reusing the micromotors for pollutant degradation applications.

Figure 12. Synthesis scheme of Vis-LDM based on BiOI/AgI/Fe_3O_4 doped with Au. Reprinted with permission from (42) (Copyright © 2020 WILEY-VCH).

In recent studies, a viable method to facilitate the reuse of Vis-LDM has been the addition of magnetic response capabilities, allowing for the easy recovery of the micromotors by external magnetic stimuli (42,45). Regarding stability, the heterojunction has emerged as the most effective approach to protect Vis-LDM from environmental factors and irradiation to which they are exposed (77).

Adaptability to adverse environmental conditions, namely extreme salinity or pH of the environment, is essential for the development of more efficient Vis-LDM. For this it is also necessary to guarantee the chemical stability of the materials used. Jiang and collaborators (93) described Vis-LDM with good stability that conferred the ability to adapt to complex external environments, such as those with high salinity. They adjusted the energy bandgap of rutile TiO_2 to generate photogenerated e^+/h^- pairs under visible light and deposited Pt nanoparticles and polyaniline on the surface of TiO_2 microspheres to facilitate movement in ion-rich environments. The innovation lays in modifying the surface of the Vis-LDM with polymers for ion tolerance, ensuring the integrity of photogenerated electron transport. Conductive polyaniline was chosen as the coating, acting as a barrier against ion penetration and maintaining the transport of photogenerated electron holes (Figure 13a). The operating mechanism of the rS-TiO_2@Pt/PANI micromotors is illustrated in Figure 13b. Under visible light illumination, a redox reaction occurs on the illuminated side of the Vis-LDM, inducing movement through the asymmetric distribution of byproducts. These new Vis-LDM

View Article Online
DOI: 10.1039/D4VA00230J

exhibited electrophoretic movement in NaCl solutions with concentrations up to 0.1 mol/L, reaching a speed of 0.47 μm/s without the need for additional chemical fuels. The propulsion of the micromotors was generated exclusively by water splitting under visible light illumination, offering several advantages over traditional micromotors, such as biocompatibility and the ability to operate in high ionic strength environments.

Figure 13. Schematics demonstrating: a) photoelectrochemical reaction that occurs on the surface of the micromotor; b) micromotor propulsion under visible light illumination. Adapted from (93) (Licensed under an open-access Creative Commons CC BY 4.0 license).

Rh_2O_3-Au nanorods powered by visible light (101) were indicated for use in adverse pH conditions due to their demonstrated resistance to strong acids and bases. This resistance was attributed to the chemical properties of their constituents. The choice of Au, a noble metal with high resistance to corrosion and chemical reactions, which does not easily react with strongest acids and bases, combined with the selection of Rh_2O_3, a stable compound with strong bonds and a crystalline structure resistant to strong acids and bases, resulted in Vis-LDM nanorods with high chemical resistance and stability, making them suitable for adverse pH conditions. Additionally, the Rh_2O_3 formed a heterojunction with Au, allowing the Rh_2O_3-Au nanorod to move in the direction of the hemisphere where Au was, under visible light via self-electrophoresis, with the speed increasing with light intensity (maximum reached 28.5 μm/s with 10 % H_2O_2).

Similarly, new Vis-LDM based gC_3N_4 doped with Fe^{3+} (FCN) with enhanced photocatalytic capabilities under extreme pH conditions have been described (102). In the presence of H_2O_2, these new Vis-LDM demonstrated the ability to degrade tetracycline (50 mg/L) with a constant rate of 0.034 min^{-1} at acidic pH (3.1) and 0.091 min^{-1} at alkaline pH within the first 20 minutes, corresponding to a degradation percentage exceeding 85 %. The Fe^{3+} doping facilitated the formation of Fe-N bonds, similar to those found in biologically rich residues with enzyme centers containing Fe-N, which enhanced e^+/h^- pair absorption and separation, accelerated the Fe^{2+}/Fe^{3+} catalytic cycles, and served as active sites for the production of photon-generated carriers (Figure 14). This study demonstrated a simple and cost-effective approach to synthesizing efficient visible-light-driven photocatalysts for the photo-Fenton reaction, overcoming the challenge of low catalytic activity under alkaline conditions.

Figure 14. Representative scheme of the photodegradation process that occurred: a) in an acidic environment and b) in an alkaline environment. Reprinted with permission from (102) (Copyright © 2022 WILEY-VCH).

In summary, the adaptation of Vis-LDM to adverse environmental conditions, achieved by the stability of the materials, can improve photocatalytic efficiency in any less favorable condition, allowing them to operate consistently and effectively.

View Article Online
DOI: 10.1039/D4VA00230J

Regarding the collective behavior of Vis-LDM, it can enhance their efficiency in several ways. Operating collectively, Vis-LDM can synchronize their movements, distribute capacities evenly, and increase their load carrying capacity. This results in more efficient use of energy and resources, and enables them to perform complex tasks more effectively than if they were operating individually. In essence, the collective behavior of Vis-LDM can make them more efficient and versatile in their photocatalytic activity. For example, a study described Vis-LDM inspired by the swarming behavior of bacteria, aiming for cooperation and communication among them, as well as the cooperative transport of large loads (103). The Vis-LDM based on $BiVO_4$ and $GO/BiVO_4$, were synthesized by a hydrothermal method, demonstrating self-propulsion without the need for fuel and dynamic collective "predator-prey" behavior using the photocatalytic reaction of $BiVO_4$. A unique behavior was observed: smaller (2 μm) $BiVO_4$ particles ("predators") were attracted to larger (10 μm) $GO/BiVO_4$ particles ("prey") under weak light (0.2 W cm^{-2}), managing to escape under intermediate light (0.6 W cm^{-2}) (Figure 15a-c). The average speed of the Vis-LDM increased with light intensity; however, the $GO/BiVO_4$ micromotor did not move under weak light due to the higher drag force of the fluid. Doping with GO accelerated the photocatalytic reaction, resulting in higher speed under intense light. Under weak light, the electric field generated by the photocatalytic reaction caused an electroosmotic flow that attracted the smaller $BiVO_4$ micromotors to the larger ones. Under intermediate light, self-diffusiophoresis dominated, dispersing the $BiVO_4$ micromotors (Figure 15d). By adjusting the light intensity, it was possible to control the formation and dispersion of micromotor clusters. This mechanism achieved excellent catalytic performance, with an apparent rate.

Figure 15. Schematic illustration showing: a,b) the movement of $BiVO_4$ particles around the $GO/BiVO_4$ micromotor under light irradiation of 0.2 Wcm^{-2} and 0.6 Wcm^{-2}, respectively; c) optical microscope images showing the aggregation and disaggregation process of $BiVO_4$ micromotors (scale bar: 5 μm); d,e) Schematic illustration of the aggregation and disassembly behavior and based on the competition between the mechanism of autodiffusiophoresis and electroosmosis, respectively. Adapted from (103) (Licensed under an open-access Creative Commons CC BY 4.0 license).

This cooperative effect demonstrated a new capability of Vis-LDM in terms of adaptability and controllable behavior. Specifically, the ability to control the formation and dispersion of clusters by adjusting light intensity allows for precise manipulation of micromotor activity, optimizing their efficiency for specific tasks. Furthermore, the dynamic response of micromotors to different light intensities creates a form of adaptation, making Vis-LDM more versatile and effective in different environments. In terms of photocatalytic performance, the micromotors, including $BiVO_4$ and $GO/BiVO_4$ variants, showed high efficiency in RhB dye degradation. Under light intensities of 0.2 W cm^{-2} and 0.6 W cm^{-2}, the Vis-LDM achieved a 97.4 % degradation rate, in 30 minutes. UV-Vis spectroscopy confirmed effective dye degradation, as indicated by the decreasing absorption peak of RhB.

View Article Online
DOI: 10.1039/D4VA00230J

The degradation followed first-order kinetics with an apparent rate constant of 0.076 min^{-1}. The normalized rate constant of 1.87 × 10^{-2} $Lm^{-2}s^{-1}$ highlighted the micromotors strong performance in organic pollutant removal. Overall, the $BiVO_4$-based Vis-LDM demonstrated excellent photocatalytic efficiency.

Table 2 compiles the main advances in photocatalytic Vis-LDM applied to the degradation of environmental pollutants, with a brief summary of each solution used to address specific limitations encountered.

Table 2 - Summary of the recent solutions used to address specific limitations of Vis-LDM photocatalysts.

Challenges	Recent solutions	References
Ecological, sustainable and biocompatible variants of Vis-LDM		
Absence of fuel	**Optimizing the morphology to obtain crystalline Vis-LDM** with greater exposure of crystal facets that enhances photocatalytic activity ({110} and {111}) **Hybridization of Vis-LDM** with inorganic molds and organic polymers, such as thiophene and triazine units, guides movement and increases photocatalytic activity.	(21,84)
Biofuels (*e.g* glucose, and tannic acid)	**Impregnation of Vis-LDM with an enzymatic system (i.e., GOx/Cat)**: GOx uses glucose to produce H_2O_2, which is then broken down by Cat, generating active radicals and oxygen bubbles that propel the nanoparticles. **Doping of Vis-LDM with GO**: This improves photocatalytic activity by enhancing charge separation, increasing surface area, improving light absorption, and introducing local photothermal effects.	(13,75,88)
Natural resources for Vis-LDM production	**Using biological resources rich in carbon and phenolic units (like lignin or** halloysite**)** for the production of functional Vis-LDM. **Creating Vis-LDM inspired by biological motors** involves using modified cellulose nanocrystals or NiMn-CLDH nanosheets with ascorbic acid. For example, NiMn-CLDH nanosheets have built-in oxidase/peroxidase activity and, with ascorbic acid, form a 3D structure with more reactive sites, enhancing photonic efficiency. **Impregnation of Vis-LDM with a molecular photosensor like** spiropyran **that changes spatial conformation upon exposure to specific wavelengths of light, enabling light-controlled substitution of the motor mechanism.**	(81,82,95–97)
Combination with Other External Parameters	**Creating hybrid-powered Vis-LDM using magnetic materials** such as Fe_3O_4 that enhanced the photocatalytic Fenton reaction, increasing the production of reactive species for the degradation of environmental pollutants.	(31,74,86,89)
Doping	**Doping with noble metals (Pt and Au)**: This enhances the separation and movement of photogenerated carriers at semiconductor interfaces and improves visible light absorption due to their ability to accept electrons as cocatalysts and their localized surface plasmon resonance effect.	(29,79,85,99)
Heterojunction formation	**Creating Vis-LDM by heterojunction with two semiconductors** (*e.g* ZnO/BiOI; ZnO/SnS; TiO_2/CdS; Ag_3PO_4/gC_3N_4) that enhances photocatalytic activity by facilitating charge separation. The electric field at their interface helps separate e^+/h^- pairs, reducing recombination and increasing	(30,44,76)

	reaction efficiency. Additionally, using semiconductors with complementary band gaps broadens light absorption, further boosting photonic performance.	
Crystallinity adjustments	**Optimizing the morphology to obtain crystalline Vis-LDM** with greater exposure of crystal facets that enhances photocatalytic activity ({110} and {111})	(21,36,80,100)
Enhancing Stability, Reusability and Collective Behavior		
Reuse	**Creating hybrid-powered Vis-LDM using magnetic materials** such as Fe_3O_4 that allow programmable and controllable propulsion in response to magnetic fields for recovery and reuse	(42,45,77)
Collective Behavior	**Creating Vis-LDM with the same photocatalytic base (ie. BiO4), but different diameters** originated by doping with GO in order to obtain smaller $BiVO_4$ particles ("predators") that are attracted by larger GO/$BiVO_4$ particles ("prey") giving rise to a dynamic collective movement	(103)
Stability	**Modifying the surface of Vis-LDM with polymers like polyaniline** to improve ion tolerance, protect photogenerated electron transport, act as a barrier against ion penetration, and maintain stability under varying salinity and pH conditions.	(93,101,102)

View Article Online
DOI: 10.1039/D4VA00230J

5. Conclusions

This review addresses recent advances in Vis-LDM photocatalysts, highlighting their great potential to effectively and sustainably mitigate environmental pollution. It focuses on recent achievements for tackling the limitations identified in the field, and provides an overview of materials, synthesis techniques, and applications in the removal of pollutants. The choice of materials such as gC_3N_4 (30–32), Cu_2O (33–36), Ag_3PO_4 (21,29,37–39), and BiOI (44–48) is crucial for the efficacy of the photocatalysts, despite the challenges entailed by these materials such as rapid pair recombination and low charge efficiency. Semiconductors like TiO_2 and ZnO continue to be extensively explored despite their limitations in absorbing visible light. Strategies such as doping (51,52), forming heterojunctions (49,50) and dye sensitizing (53) have been used to improve these properties. However, additional challenges like durability, dependence on toxic chemical fuels, stability, and recovery of Vis-LDM still require future efforts to overcome them. Innovations in photocatalytic materials, surface modifications, and synthesis conditions have been explored to optimize the application of Vis-LDM in the photodegradation of pollutants.

Recent advances in fuelless Vis-LDM relied on inorganic-organic hybrid structures (84) and crystalline materials with adjustable morphologies that increase the exposure of the most active crystalline facets (21). While these modifications extend their applications and improve sustainability, they may reduce the efficiency of light energy conversion, decreasing movement and photonic efficacy. Alternatives with biofuels such as water, glucose, and tannic acid (36) have been explored due to their lower toxicity, although they also face logistical and economic challenges, such as the need for continuous supply and the complexity of storage and delivery.

The transition to natural/biological materials has been explored to promote sustainability and environmental efficiency in Vis-LDM. Using natural resources like lignin (81), cellulose nanocrystals (82), and halloysite (87) a sustainable approach to producing these devices has been developed. These materials offer biocompatibility and resource reuse, allowing the integration of enzymes and biomolecules for innovative propulsion mechanisms (97).. However, these new Vis-LDM face challenges in energy conversion efficiency and the integration of biological and inorganic components, requiring more appropriate synthesis techniques.

Strategies to increase the efficiency and versatility of Vis-LDM, such as doping, heterojunction formation, and crystallinity adjustments, have been described in this review.

The stability and reuse of Vis-LDM are limitations that must be overcome to extend their useful lifetime, improve efficiency, and reduce costs. Recent advances, including the integration of magnetic capabilities to facilitate the recovery of motors and the development of materials resistant to adverse conditions, have been described in this review.

View Article Online
DOI: 10.1039/D4VA00230J

Adapting to environmental conditions and the collective behavior of Vis-LDM have been explored challenges to improve their catalytic efficiency in adverse conditions. Collective work among Vis-LDM demonstrated the possibility of synchronized movements and uniform distribution of capabilities, increasing operational efficiency. This allowed Vis-LDM to adapt to environmental conditions while maintaining controllable and stable behavior.

Photocatalytic Vis-LDM have demonstrated strong effectiveness in pollutant removal across various applications. When addressing bacterial biofilms, these micromotors excel, particularly when in motion, leading to significant reductions in both biofilm viability and thickness. In the degradation of organic pollutants, such as dyes, these micromotors achieve high removal rates, with enhancements from additives like hydrogen peroxide further boosting efficiency. For microplastic remediation, Vis-LDM effectively reduce plastics to smaller fragments, with their magnetic properties aiding in recovery and continued use. Advances in photocatalytic materials, including Fe-doped ZnO-CdS and Cu_2O-TiO_2 composites, have further improved degradation performance, underscoring the versatility and enhanced capabilities of these technologies in environmental cleanup.

In summary, Vis-LDM demonstrate enormous potential for the effective photodegradation of pollutants, with recent advances indicating significant progress in overcoming challenges and expanding possibilities for future practical applications. However, it is important to note that despite these advances, definitive solutions to these limitations are still needed.

Future perspective

Despite Vis-LDM representing an emerging research area poised to revolutionize the field of photodegradation of pollutants, significant technical and scientific challenges still need to be overcome for this technology to reach its full maturity and commercialization. Specifically, scalability, cost-effectiveness, and environmental compatibility remain key concerns. While Vis-LDM have shown effectiveness on a small scale in laboratory settings, scaling up their production and deployment to tackle real-world environmental challenges presents a substantial obstacle. Developing manufacturing processes capable of producing these robots in large quantities while maintaining quality and consistency is essential for practical implementation on a larger scale.

Cost-effectiveness is another critical factor requiring attention. Currently, the production and deployment of Vis-LDM can be costly, limiting their accessibility and viability for wide adoption. Finding ways to reduce production costs without compromising the performance and reliability of these robots is essential to make them economically feasible for environmental cleanup applications. Furthermore, ensuring the environmental compatibility of Vis-LDM is crucial. It is important to evaluate the potential ecological impacts of deploying these robots in natural environments and mitigate any adverse effects on ecosystems. Designing Vis-LDM with biodegradable materials or incorporating mechanisms for safe disposal after use can help minimize their environmental footprint. Addressing these

View Article Online
DOI: 10.1039/D4VA00230J

challenges will be crucial to unlock the full potential of Vis-LDM in environmental cleanup and realize their benefits for sustainable development and environmental protection. Collaboration among researchers, engineers, and industry stakeholders will be essential to overcome these obstacles and drive innovation in this field.

The incorporation of programmable routes and precise navigation would also be beneficial to allow Vis-LDM to access hard to reach areas with accuracy and autonomy, enhancing their versatility and ability to navigate challenges without causing damage due to their flexible nature. In order to locate and remove the most hazardous contaminants from wastewater, Vis-LDM should exhibit selective behavior. The molecular imprinting technique, where a molecule (template) is imprinted onto a material (matrix) during preparation, followed by template removal to leave complementary cavities allowing selective adsorption, presents a potential solution to this problem. However, current literature on selective micro/nanomotors has primarily focused on those driven by magnetic fields, with limited research on light-driven micro/nanomotors, particularly Vis-LDM.

Regarding the disadvantage the limited navigation range of Vis-LDM, this becomes particularly challenging when they are required to operate in large volumes of water, often measured in cubic meters. Developing hybrid Vis-LDM that integrate different propulsion mechanisms, such as chemical and magnetic, could offer navigation control by directed light or magnetic fields, resulting in much greater travel distances. Alternatively, operating a large volume of fluid through small flow systems, where limited range is less of an issue or directed light is of easy implementation, represents another potential solution to this limitation.Gravitational sedimentation of Vis-LDM is another possible significant limitation, associated with all micromotors in general, having the potential to affect greatly the physical characteristics of movement and the catalytic properties of these devices. This issue is rarely accounted for in the literature, as corroborated by the fact that none of the recent papers reviewed here tackle it. It is desirable that researchers include the assessment of the settling properties of LDM in their studies. In case it is found necessary to mitigate the impact of sedimentation, some strategies can be adopted. One possible approach is to develop Vis-LDM with properties that minimize sedimentation, such as rougher surfaces that enhance suspension, or the incorporation of stabilizing agents. External techniques, such as electric and magnetic fields, can also help keep the motors suspended and evenly distributed within the fluid. Adjusting operational conditions, such as the fluids viscosity and density, can reduce the sedimentation rate and improve the overall efficiency of the Vis-LDM in pollutant treatment. Reducing the density of Vis-LDM is also crucial, as it can delay sedimentation; this can be achieved, for example, through the synthesis of hollow structures.

Future research efforts should focus on testing these robots in real world contaminated samples to assess their practical feasibility and address navigation challenges. In conclusion, overcoming these challenge through collaborative research and innovation will be essential

View Article Online
DOI: 10.1039/D4VA00230J

to fully harnessing the potential of Vis-LDM for environmental remediation, contributing to a cleaner and healthier environment globally.

Author contributions:

Conceptualization, writing—review and editing, V.R.A.F. and M.A.A. All authors have read and agreed to the published version of the manuscript.

Acknowledgements:

This work was financed by the Portuguese Foundation for Science and Technology (FCT) through financial support to CIQUP (UIDB/00081/2020 and UIDP/00081/2020) and to IMS (LA/P/0056/2020).

References

1. Ferreira VRA, Azenha MA. Recent Advances in Light-Driven Semiconductor-Based Micro/Nanomotors: Optimization Strategies and Emerging Applications. Molecules. 2024;29(5):23699–731. https://doi.org/10.3390/molecules29051154
2. Jurado-Sánchez B, Wang J. Micromotors for environmental applications: a review. Environ Sci Nano. 2018;5(7):1530–44. https://doi.org/10.1039/C8EN00299A
3. Ye H, Wang Y, Xu D, Liu X, Liu S, Ma X. Design and fabrication of micro/nano-motors for environmental and sensing applications. Appl Mater Today. 2021;23(2):101007-21. https://doi.org/10.1016/j.apmt.2021.101007
4. Zeng X, Yang M, Liu H, Zhang Z, Hu Y, Shi J, et al. Light-driven micro/nanomotors in biomedical applications. Nanoscale. 2023;15(46):18550–70. https://doi.org/10.1039/D3NR03760F
5. Yuan K, Bujalance-Fernández J, Jurado-Sánchez B, Escarpa A. Light-driven nanomotors and micromotors: envisioning new analytical possibilities for bio-sensing. Microchim Acta. 2020;187(10):132–44. https://doi.org/ 10.1007/s00604-020-04541-y
6. Jurado-Sánchez B, Pacheco M, Maria-Hormigos R, Escarpa A. Perspectives on Janus micromotors: Materials and applications. Appl Mater Today. 2017;9(2):407–18. http://dx.doi.org/10.1016/j.apmt.2017.09.005
7. Somasundar A, Sen A. Chemically Propelled Nano and Micromotors in the Body: Quo Vadis? Small. 2021;17(5):1–7. https://doi.org/10.1002/smll.202007102
8. Wu Y, Yakov S, Fu A, Yossifon G. A Magnetically and Electrically Powered Hybrid Micromotor in Conductive Solutions: Synergistic Propulsion Effects and Label-Free Cargo Transport and Sensing. Adv Sci. 2023;10(8):1–13. https://doi.org/10.1002/advs.202204931
9. Xiao Y, Zhang J, Fang B, Zhao X, Hao N. Acoustics-Actuated Microrobots. Micromachines. 2022;13(3):481–96. https://doi.org/10.3390/mi13030481

View Article Online
DOI: 10.1039/D4VA00230J

10. Wang H, Bisoyi HK, Zhang X, Hassan F, Li Q. Visible Light-Driven Molecular Switches and Motors: Recent Developments and Applications. Chem - A Eur J. 2022;28(18):1877–99. https://doi.org/10.1002/chem.202103906

11. Zhou H, Mayorga-Martinez CC, Pané S, Zhang L, Pumera M. Magnetically Driven Micro and Nanorobots. Chem Rev. 2021;121(8):4999–5041. https://doi.org/10.1021/acs.chemrev.0c01234

12. Soto F, Karshalev E, Zhang F, Esteban Fernandez de Avila B, Nourhani A, Wang J. Smart Materials for Microrobots. Chem Rev. 2022;122(5):5365–403. https://doi.org/10.1021/acs.chemrev.0c00999

13. Yang Q, Xu H, Wen H, Zhao H, Liu X, Cai Y, et al. Graphene oxide induced enhancement of light-driven micromotor with biocompatible fuels. Appl Mater Today. 2021;22(12):100943–1010036. https://doi.org/10.1016/j.apmt.2021.100943

14. Alageshwaramoorthy K, Mannu P, Mahalingam S, Nga TTT, Chang HW, Masuda Y, et al. Synthesis and characterization of visible-light-driven novel CuTa2O6 as a promising practical photocatalyst. Front Chem. 2023;11(June):1–12. https://doi.org/10.3389/fchem.2023.1197961

15. Liang X, Mou F, Huang Z, Zhang J, You M, Xu L, et al. Hierarchical Microswarms with Leader–Follower-Like Structures: Electrohydrodynamic Self-Organization and Multimode Collective Photoresponses. Adv Funct Mater. 2020;30(16):1908602–20. https://doi.org/10.1002/adfm.201908602

16. Villa K, Novotný F, Zelenka J, Browne MP, Ruml T, Pumera M. Visible-Light-Driven Single-Component BiVO4 Micromotors with the Autonomous Ability for Capturing Microorganisms. ACS Nano. 2019;13(7):8135–45. https://doi.org/10.1021/acsnano.9b03184

17. Wang Y, Li Z, Solovev AA, Huang G, Mei Y. Light-controlled two-dimensional TiO2 plate micromotors. RSC Adv. 2019;9(50):29433–9. https://doi.org/10.1039/C9RA06426E

18. Yu T, Athanassiadis AG, Popescu MN, Chikkadi V, Güth A, Singh DP, et al. Microchannels with self-pumping walls. ACS Nano. 2020;14(10):13673–80. https://doi.org/10.1021/acsnano.0c05826

19. Feng K, Zhang L, Gong J, Qu J, Niu R. Visible light triggered exfoliation of COF micro/nanomotors for efficient photocatalysis. Green Energy Environ. 2023;8(2):567–78. https://doi.org/10.1016/j.gee.2021.09.002

20. Dong R, Cai Y, Yang Y, Gao W, Ren B. Photocatalytic Micro / Nanomotors : from Construction to Applications. ACS Publ. 2018;2(3):133-152. https://doi.org/10.1021/acs.accounts.8b00249.

21. Rojas D, Kuthanova M, Dolezelikova K, Pumera M. Facet nanoarchitectonics of visible-light driven Ag3PO4 photocatalytic micromotors: Tuning motion for biofilm eradication. NPG Asia Mater. 2022;14(1):236–55. https://doi.org/10.1038/s41427-022-00409-0

View Article Online
DOI: 10.1039/D4VA00230J

22. Wang J, Dong R, Yang Q, Wu H, Bi Z, Liang Q, et al. One body, two hands: Photocatalytic function- and Fenton effect-integrated light-driven micromotors for pollutant degradation. Nanoscale. 2019;11(35):16592–8. https://doi.org/10.1039/C9NR04295D
23. Zhou D, Zhuang R, Chang X, Li L. Enhanced Light-Harvesting Efficiency and Adaptation: A Review on Visible-Light-Driven Micro/Nanomotors. Research. 2020; 2020(25) 6821595-608. https://doi.org/10.34133/2020/6821595
24. Kong L, Mayorga-Martinez CC, Guan J, Pumera M. Photocatalytic Micromotors Activated by UV to Visible Light for Environmental Remediation, Micropumps, Reversible Assembly, Transportation, and Biomimicry. Small. 2020;16(27):1–14. https://doi.org/10.1002/smll.201903179
25. Safdar M, Simmchen J, Jänis J. Light-driven micro- and nanomotors for environmental remediation. Environ Sci Nano. 2017;4(8):1602–16. DOI https://doi.org/10.1039/C7EN00367F
26. Villa K, Pumera M. Fuel-free light-driven micro/nanomachines: Artificial active matter mimicking nature. Chem Soc Rev. 2019;48(19):4966–78. https://doi.org/10.1039/C9CS00090A
27. Rayaroth MP, Lee G, Chang YS. Recent developments in graphitic carbon nitride (g-C3N4) applications in micromotors. Results Eng. 2024;22(1):102244–56. https://doi.org/10.1016/j.rineng.2024.102244
28. Wang Y, Ding M, Li Z, Li M. Visible light photocatalytic degradation of dyes by Ag3PO4/g-C3N4/CQDs composite. Surfaces and Interfaces. 2024;44(20):103585. https://doi.org/10.1016/j.surfin.2023.103585
29. Dai Y, Wang Y, Zuo G, Kong J, Guo Y, Sun C, et al. Photocatalytic degradation mechanism of phenanthrene over visible light driven plasmonic Ag/Ag3PO4/g-C3N4 heterojunction nanocomposite. Chemosphere. 2022;293(21):133575. https://doi.org/10.1016/j.chemosphere.2022.133575
30. Song X, Tao Y, Liu J, Lin J, Dai P, Wang Q, et al. Photocatalytic-induced bubble-propelled isotropic g-C3N4-coated carbon microsphere micromotors for dynamic removal of organic pollutants. RSC Adv. 2022;12(21):13116–26. https://doi.org/10.1039/D2RA01577C
31. Zheng C, Song X, Gan Q, Lin J. High-efficiency removal of organic pollutants by visible-light-driven tubular heterogeneous micromotors through a photocatalytic Fenton process. J Colloid Interface Sci. 2023;630(12):121–33. https://doi.org/10.1016/j.jcis.2022.10.021
32. Rayaroth MP, Oh D, Lee CS, Kumari N, Lee IS, Chang YS. Carbon-nitride-based micromotor driven by chromate-hydrogen peroxide redox system: Application for removal of sulfamethaxazole. J Colloid Interface Sci. 2021;597(2):94–103. https://doi.org/10.1016/j.jcis.2021.03.164
33. Zhou D, Li YC, Xu P, McCool NS, Li L, Wang W, et al. Visible-light controlled catalytic Cu2O-Au micromotors. Nanoscale. 2017;9(1):75–8. https://doi.org/10.1039/C6NR08088J

View Article Online
DOI: 10.1039/D4VA00230J

34. Wang J, Wu H, Liu X, Liang Q, Bi Z, Wang Z, et al. Carbon-Dot-Induced Acceleration of Light-Driven Micromotors with Inherent Fluorescence. Adv Intell Syst. 2020;2(3):1–6. https://doi.org/10.1002/aisy.201900159

35. Wang Q, Dong R, Yang Q, Wang J, Xu S, Cai Y. Highly efficient visible-light-driven oxygen-vacancy-based Cu2+1O micromotors with biocompatible fuels. Nanoscale Horizons. 2020;5(2):325–30. DOI https://doi.org/10.1039/C9NH00592G

36. Liu W, Chen X, Ding X, Long Q, Lu X, Wang Q, et al. Visible-light-driven cuprous oxide nanomotors with surface-heterojunction-induced propulsion. Nanoscale Horizons. 2021;6(3):238–44. https://doi.org/10.1039/D0NH00663G

37. Al Kausor M, Gupta S Sen, Chakrabortty D. Ag3PO4-based nanocomposites and their applications in photodegradation of toxic organic dye contaminated wastewater: Review on material design to performance enhancement. J Saudi Chem Soc. 2020;24(1):20–41. https://doi.org/10.1016/j.jscs.2019.09.001

38. Wang Y, Feng W, Gong A, Zhang W, Qiu L, Chen Y, et al. Photocatalytic Degradation of Polycyclic Aromatic Hydrocarbons by Ag3PO4/MoS2 Composite. Catal Letters. 2024;154(7):3574–93. https://doi.org/10.1007/s10562-024-04612-2

39. Li X, Xu P, Chen M, Zeng G, Wang D, Chen F, et al. Application of silver phosphate-based photocatalysts: Barriers and solutions. Chem Eng J. 2019;366(1):339–57. https://doi.org/10.1016/j.cej.2019.02.083

40. Panthi G, Gyawali KR, Park M. Towards the enhancement in photocatalytic performance of ag3po4 nanoparticles through sulfate doping and anchoring on electrospun nanofibers. Nanomaterials. 2020;10(5):36–49. https://doi.org/10.3390/nano10050929

41. Dong R, Hu Y, Wu Y, Gao W, Ren B, Wang Q, et al. Visible-light-driven BiOI-based janus micromotor in pure water. J Am Chem Soc. 2017;139(5):1722–5. https://doi.org/10.1021/jacs.6b09863

42. Zhan Z, Wei F, Zheng J, Yin C, Yang W, Yao L, et al. Visible light driven recyclable micromotors for "on-the-fly" water remediation. Mater Lett. 2020;258(3):126825–38. https://doi.org/10.1016/j.matlet.2019.126825

43. Huang Y, Xu H, Yang H, Lin Y, Liu H, Tong Y. Efficient Charges Separation Using Advanced BiOI-Based Hollow Spheres Decorated with Palladium and Manganese Dioxide Nanoparticles. ACS Sustain Chem Eng. 2018;6(2):2751–7. https://doi.org/10.1021/acssuschemeng.7b04435

44. Zhou H, Wu B, Dekanovsky L, Wei S, Khezri B, Hartman T, et al. Integration of BiOI nanosheets into bubble-propelled micromotors for efficient water purification. FlatChem. 2021;30(55):100294–303. https://doi.org/10.1016/j.flatc.2021.100294

45. Liu Y, Li J, Li J, Yan X, Wang F, Yang W, et al. Active magnetic Fe3+-doped BiOBr micromotors as efficient solar photo-fenton catalyst. J Clean Prod. 2020;252(3):119573–88. https://doi.org/10.1016/j.jclepro.2019.119573

46. Khairudin K, Abu Bakar NF, Osman MS. Magnetically recyclable flake-like BiOI-Fe3O4microswimmers for fast and efficient degradation of microplastics. J Environ Chem Eng. 2022;10(5):108275–90. https://doi.org/10.1016/j.jece.2022.108275

View Article Online
DOI: 10.1039/D4VA00230J

47. Zhang Y, Li Y, Yuan Y. Carbon Quantum Dot-Decorated BiOBr/Bi2WO6Photocatalytic Micromotor for Environmental Remediation and DFT Calculation. ACS Catal. 2022;12(22):13897–909. https://doi.org/10.1021/acscatal.2c04149
48. Gong D, Li Y, Zhou H, Gu B, Celi N, Zhang D, et al. BiOX-loaded biohybrid magnetic microrobots for enhanced photocatalysis under visible light. Appl Mater Today. 2023;35(2):26–41. https://doi.org/10.1016/j.apmt.2023.101915
49. Varun Sridhar, Byung-Wook Park, Surong Guo, Peter A. van Aken MS. Multiwavelength-Steerable Visible-Light-Driven Magnetic CoO−TiO2 Microswimmers. ACS Appl Mater Interfaces. 2020;12(2):24149−24155. https://dx.doi.org/10.1021/acsami.0c06100
50. Étude O'Neel-Judy, Dylan Nicholls, John Castañeda JGG. Light-Activated Multi-Semiconductor Hybrid Microswimmers. Small. 2018;14(2):1801860–9. https://doi.org/10.1002/smll.201801860
51. Wang X, Sridhar V, Guo S, Talebi N, Miguel-López A, Hahn K, et al. Fuel-Free Nanocap-Like Motors Actuated Under Visible Light. Adv Funct Mater. 2018;28(25):1705862–99. https://doi.org/10.1002/adfm.201705862
52. Jiang Z, Yu X. Performance of Visible-Light-Driven Photocatalytic Pavement in Reduction of Motor Vehicles' Exhaust Gas. Transp Res Rec. 2020;2674(11):512–9. http://dx.doi.org/10.1177/0361198120947084
53. Zheng J, Dai B, Wang J, Xiong Z, Yang Y, Liu J, et al. Orthogonal navigation of multiple visible-light-driven artificial microswimmers. Nat Commun. 2017;8(1):1–7. http://dx.doi.org/10.1038/s41467-017-01778-9
54. Khlyustova A, Sirotkin N, Kusova T, Kraev A, Titov V, Agafonov A. Doped TiO2: The effect of doping elements on photocatalytic activity. Mater Adv. 2020;1(5):1193–201. https://doi.org/10.1039/D0MA00171F
55. Mohtar SS, Aziz F, Ismail AF, Sambudi NS, Abdullah H, Rosli AN, et al. Impact of doping and additive applications on photocatalyst textural properties in removing organic pollutants: A review. Catalysts. 2021;11(10):1–31. https://doi.org/10.3390/catal11101160
56. Xu L, Mou F, Gong H, Luo M, Guan J. Light-driven micro/nanomotors: From fundamentals to applications. Chem Soc Rev. 2017;46(22):6905–26. https://doi.org/10.1039/C7CS00516D
57. Piątkowska A, Janus M, Szymański K, Mozia S. C-,n-and s-doped tio2 photocatalysts: A review. Catalysts. 2021;11(1):1–56. https://doi.org/10.3390/catal11010144
58. Cui X, Li J, Ng DHL, Liu J, Liu Y, Yang W. 3D hierarchical ACFs-based micromotors as efficient photo-Fenton-like catalysts. Carbon N Y. 2020;158:738–48. https://doi.org/10.1016/j.carbon.2019.11.048
59. Villa K. Exploring innovative designs and heterojunctions in photocatalytic micromotors. Chem Commun. 2023;59(54):8375–83. DOI https://doi.org/10.1039/D3CC01634J

View Article Online
DOI: 10.1039/D4VA00230J

60. Wolff N, Ciobanu V, Enachi M, Kamp M, Braniste T, Duppel V, et al. Advanced Hybrid GaN/ZnO Nanoarchitectured Microtubes for Fluorescent Micromotors Driven by UV Light. Small. 2020;16(2):1–10. https://doi.org/10.1002/smll.201905141
61. Zhao W, Li Y, Zhao P, Zhang L, Dai B, Huang H, et al. Insights into the photocatalysis mechanism of the novel 2D/3D Z-Scheme g-C3N4/SnS2 heterojunction photocatalysts with excellent photocatalytic performances. J Hazard Mater. 2021;402(20):123711–26. https://doi.org/10.1016/j.jhazmat.2020.123711
62. Choi SK, Yang HS, Kim JH, Park H. Organic dye-sensitized TiO 2 as a versatile photocatalyst for solar hydrogen and environmental remediation. Appl Catal B Environ. 2012;121(12):206–13. http://dx.doi.org/10.1016/j.apcatb.2012.04.011
63. Watanabe M. Dye-sensitized photocatalyst for effective water splitting catalyst. Sci Technol Adv Mater. 2017;18(1):705–23. http://doi.org/10.1080/14686996.2017.1375376
64. Wang L, Popescu MN, Stavale F, Ali A, Gemming T, Simmchen J. Cu@TiO2 Janus microswimmers with a versatile motion mechanism. Soft Matter. 2018;14(34):6969–73. https://doi.org/10.1039/C8SM00808F
65. Wittmann M, Ali A, Gemming T, Stavale F, Simmchen J. Semiconductor-Based Microswimmers: Attention to Detail Matters. J Phys Chem Lett. 2021;12(39):9651–6. https://doi.org/10.1021/acs.jpclett.1c02658
66. Deng Z, Mou F, Tang S, Xu L, Luo M, Guan J. Swarming and collective migration of micromotors under near infrared light. Appl Mater Today. 2018;13(33):45–53. https://doi.org/10.1016/j.apmt.2018.08.004
67. Li X, Sun YM, Zhang ZY, Feng NX, Song H, Liu YL, et al. Visible light-driven multi-motion modes CNC/TiO2 nanomotors for highly efficient degradation of emerging contaminants. Carbon N Y. 2019;155(2):195–203. https://doi.org/10.1016/j.carbon.2019.08.039
68. Wang J, Xiong Z, Zheng J, Zhan X, Tang J. Light-Driven Micro/Nanomotor for Promising Biomedical Tools: Principle, Challenge, and Prospect. Acc Chem Res. 2018;51(9):1957–65. https://doi.org/10.1021/acs.accounts.8b00254
69. Enachi M, Guix M, Postolache V, Ciobanu V, Fomin VM, Schmidt OG, et al. Light-Induced Motion of Microengines Based on Microarrays of TiO2 Nanotubes. Small. 2016;12(39):5497–505. https://doi.org/10.1002/smll.201670203
70. Wang H, Pumera M. Fabrication of micro/nanoscale motors. Chem Rev. 2015;115(16):8704–35. https://doi.org/10.1021/acs.chemrev.5b00047
71. Sridhar V, Park BW, Sitti M. Light-Driven Janus Hollow Mesoporous TiO2–Au Microswimmers. Adv Funct Mater. 2018;28(25):1704902–15. https://doi.org/10.1002/adfm.201704902
72. Nicholls D, Deverse A, Esplin R, Castañeda J, Loyd Y, Nair R, et al. Shape-Dependent Motion of Structured Photoactive Microswimmers. ACS Appl Mater Interfaces. 2018;10(21):18050–6. https://doi.org/10.1021/acsami.8b01940

View Article Online
DOI: 10.1039/D4VA00230J

73. Wang H, Potroz MG, Jackman JA, Khezri B, Marić T, Cho NJ, et al. Bioinspired Spiky Micromotors Based on Sporopollenin Exine Capsules. Adv Funct Mater. 2017;27(32):1–9. https://doi.org/10.1002/adfm.201702338
74. Shivalkar S, Yadav S, Tauheed A, Tariq M, Samanta SK, Sk MP, et al. Programmed Logic Operation-Based Controlled Movement of Self-Destructive Microbots for Toxic Pesticide Degradation. ACS Appl Eng Mater. 2023;1(11):2858–67. https://doi.org/10.1021/acsaenm.3c00383
75. Kutorglo EM, Elashnikov R, Rimpelova S, Ulbrich P, Říhová Ambrožová J, Svorcik V, et al. Polypyrrole-Based Nanorobots Powered by Light and Glucose for Pollutant Degradation in Water. ACS Appl Mater Interfaces. 2021;13(14):16173–81. https://doi.org/10.1021/acsami.0c20055
76. Zhu H, Li Y, Jiang X. Room-temperature synthesis of cuprous oxide and its heterogeneous nanostructures for photocatalytic applications. J Alloys Compd. 2019;772(25):447–59. https://doi.org/10.1016/j.jallcom.2018.09.092
77. Cui Y, Sheng X, Anusuyadevi PR, Lawoko M, Svagan AJ. Self-assembled carbon spheres prepared from abundant lignin and urea for photocatalytic and self-propelling applications. Carbon Trends. 2021;3(2):100040–52. https://doi.org/10.1016/j.cartre.2021.100040
78. Dhar P, Narendren S, Gaur SS, Sharma S, Kumar A, Katiyar V. Self-propelled cellulose nanocrystal based catalytic nanomotors for targeted hyperthermia and pollutant remediation applications. Int J Biol Macromol. 2020;158(3):1020–36. https://doi.org/10.1016/j.ijbiomac.2020.04.204
79. Jamdar M, Monsef R, Ganduh SH, Dawi EA, Jasim LS, Salavati-Niasari M. Unraveling the potential of sonochemically achieved DyMnO3/Dy2O3 nanocomposites as highly efficient visible-light-driven photocatalysts in decolorization of organic contamination. Ecotoxicol Environ Saf. 2024;269(23):115801-13. https://doi.org/10.1016/j.ecoenv.2023.115801
80. Dharmana G, Srinivasa Rao MP, Potukuchi DM. Visible light driven robust photocatalytic activity in vanadium-doped ZnO/SnS core-shell nanocomposites for decolorization of MB dye towards wastewater treatment. Inorg Nano-Metal Chem. 2022;52(8):1059–76. https://doi.org/10.1080/24701556.2022.2075386
81. Chen X, Ding X, Liu Y, Li J, Liu W, Lu X, et al. Highly efficient visible-light-driven Cu2O@CdSe micromotors adsorbent. Appl Mater Today. 2021;25 (2):101200–22. https://doi.org/10.1016/j.apmt.2021.101200
82. Li X, Zhao Y, Wang D, Du X. Dual-propelled PDA@MnO2 nanomotors with NIR light and H2O2 for effective removal of heavy metal and organic dye. Colloids Surfaces A Physicochem Eng Asp. 2023;658(22):130712–29.
83. Rao GT, Ravikumar RVSSN. Novel Fe-doped ZnO-CdS nanocomposite with enhanced visible light-driven photocatalytic performance. Mater Res Innov. 2021;25(4):215–20. https://doi.org/10.1080/14328917.2020.1774726

View Article Online
DOI: 10.1039/D4VA00230J

84. Kochergin YS, Villa K, Nemeškalová A, Kuchař M, Pumera M. Hybrid Inorganic-Organic Visible-Light-Driven Microrobots Based on Donor-Acceptor Organic Polymer for Degradation of Toxic Psychoactive Substances. ACS Nano. 2021;15(11):18458–68. https://doi.org/10.1021/acsnano.1c08136

85. Liu M, Jiang J, Tan H, Chen B, Ou J, Wang H, et al. Light-driven Au-ZnO nanorod motors for enhanced photocatalytic degradation of tetracycline. Nanoscale. 2022;14(35):12804–13. https://doi.org/10.1039/D2NR02441A

86. Feng K, Gong J, Qu J, Niu R, Gong J. Dual-Mode-Driven Micromotor Based on Foam-like Carbon Nitride and Fe3O4 with Improved Manipulation and Photocatalytic Performance. ACS Appl Mater Interfaces. 2022;14(39):44271–81. https://doi.org/10.1021/acsami.2c10590

87. Wang J, Si J, Hao Y, Li J, Zhang P, Zuo C, et al. Halloysite-Based Nanorockets with Light-Enhanced Self-Propulsion for Efficient Water Remediation. Langmuir. 2022;38(3):1231–42. https://doi.org/10.1021/acs.langmuir.1c03024

88. Ying Y, Plutnar J, Pumera M. Six-Degree-of-Freedom Steerable Visible-Light-Driven Microsubmarines Using Water as a Fuel: Application for Explosives Decontamination. Small. 2021;17(23):1–10. https://doi.org/10.1002/smll.202100294

89. Beladi-Mousavi SM, Hermanová S, Ying Y, Plutnar J, Pumera M. A Maze in Plastic Wastes: Autonomous Motile Photocatalytic Microrobots against Microplastics. ACS Appl Mater Interfaces. 2021;13(21): 25102–10. https://doi.org/10.1021/acsami.1c04559

90. Zhou X, Li Z, Tan L, Zhang Y, Jiao Y. Near-Infrared Light-Steered Graphene Aerogel Micromotor with High Speed and Precise Navigation for Active Transport and Microassembly. ACS Appl Mater Interfaces. 2020;12(20):23134–44. https://doi.org/10.1021/acsami.0c04970

91. Wang J, Gao W. Nano/microscale motors: Biomedical opportunities and challenges. ACS Nano. 2012;6(7):5745–51. https://doi.org/10.1021/nn3028997

92. Elgeti J, Winkler RG, Gompper G. Physics of microswimmers - Single particle motion and collective behavior: A review. Reports Prog Phys. 2015;78(5):56601. http://dx.doi.org/10.1088/0034-4885/78/5/056601

93. Jiang H, He X, Yang M, Hu C. Visible Light-Driven Micromotors in Fuel-Free Environment with Promoted Ion Tolerance. Nanomaterials. 2023;13(12):15987–99. https://doi.org/10.3390/nano13121827

94. Liu Y, Tang Y, Wang P, Zeng H. Carbonaceous halloysite nanotubes for the stabilization of Co, Ni, Cu and Zn in river sediments. Environ Sci Nano. 2019;6(8):2420–8. https://doi.org/10.1039/C9EN00326F

95. Xue J, Zhang M, Yong J, Chen Q, Wang J, Xu J, et al. Light-Switchable Biocatalytic Covalent-Organic Framework Nanomotors for Aqueous Contaminants Removal. Nano Lett. 2023;23(23):11243–51. https://doi.org/10.1021/acs.nanolett.3c03766

96. Ningning Xing, Yangsai Lyu, Jie Yang, Xiaolei Zhang, Yang Han, Weilin Zhao DHLN and JL. Motion-based phenol detection and degradation using 3D hierarchical AA-

View Article Online
DOI: 10.1039/D4VA00230J

NiMn-CLDHs@HNTs-Ag nanomotors. Environ Sci Nano. 2022;9(8):2815-26 https://doi.org/10.1039/D2EN00322H.

97. He Z, Li Y, Yang L, Li Y, Cao D, Wang S, et al. Sunlight-triggered prebiotic nanomotors for inhibition and elimination of pathogen and biofilm in aquatic environment. J Colloid Interface Sci. 2024;665(2):634–42. https://doi.org/10.1016/j.jcis.2024.03.163

98. Wang J, Xiong Z, Tang J. The Encoding of Light-Driven Micro/Nanorobots: from Single to Swarming Systems. Adv Intell Syst. 2021;3(4):233–48. https://doi.org/10.1002/aisy.202000170

99. Mengge Yuan, Mengqin Gong, Hai Huang, Yu Zhao YY and SW. Bubble-propelled plasmon-reinforced Pt-ZnIn2S4 micromotors for stirring-free photocatalytic water purification. Inorg Chem Front. 2022;9(22):5725-34 https://doi.org/10.1039/D2QI01291J.

100. Zeng J, Xie L, Liu T, He Y, Liu W, Zhang Q, et al. Super-Assembled Multilayered Mesoporous TiO2 Nanorockets for Light-Powered Space-Confined Microfluidic Catalysis. ACS Appl Mater Interfaces. 2023;3(1):788–99. https://doi.org/10.1021/acsami.3c19302

101. Cui D, Lyu X, Duan S, Peng Y, Wang W. Rhodium Oxide Nanorod Motors Powered by Light across the Full Visible Spectrum. ACS Appl Nano Mater. 2022;5(10):14235–40. https://doi.org/10.1021/acsanm.2c03560

102. Haoran Sun, Lijing Wang, Feng Guo, Yuxing Shi, Lingling Li, Zheng Xu, Xu Yan WS. Fe-doped g-C3N4 derived from biowaste material with Fe-N bonds for enhanced synergistic effect between photocatalysis and Fenton degradation activity in a broad pH range. J Alloys Compd. 2022;900(2):163410-19. https://doi.org/10.1016/j.jallcom.20.

103. Chen Z, Jiang J, Wang X, Zhang H, Song B, Dong B. Visible light-regulated BiVO4-based micromotor with biomimetic 'predator-bait' behavior. J Mater Sci [Internet]. 2022;57(6):4092–103. https://doi.org/10.1007/s10853-022-06882-w

View Article Online
DOI: 10.1039/D4VA00230J

Data Availability Statement

The data supporting this review are available through the literature, with many documents accessible through open access.

View Article Online
DOI: 10.1039/D4VA00230J

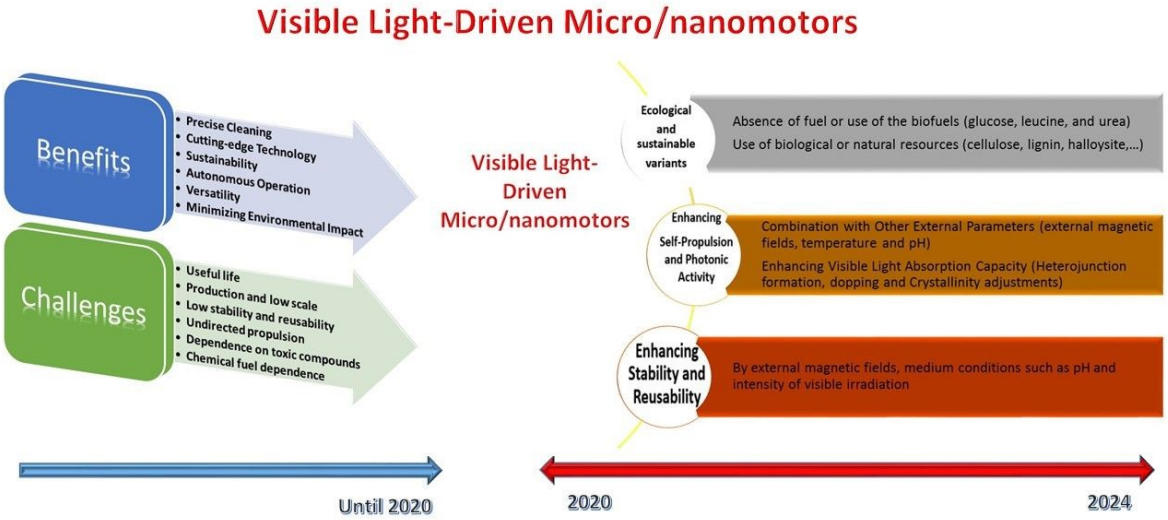

Graphical abstract

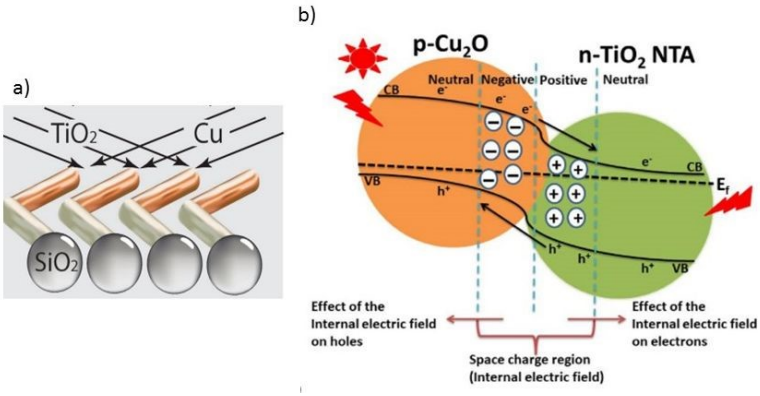

Figure 1. Representative scheme: a) of Vis-LDM and b) about charge transfer in a heterostructure with a p–n junction. Reproduced with permission from (50) (Copyright © 2020 WILEY-VCH).

View Article Online
DOI: 10.1039/D4VA00230J

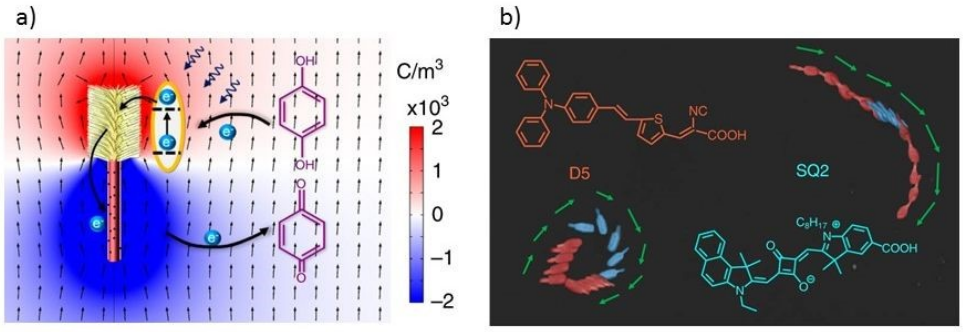

Figure 2. Representation of: (a)dye-sensitized nanotree, activated by a photoelectrochemical reaction with numerically simulated charge distribution (displayed in a color map); (b) movement generated by nanotrees sensitized with the dyes D5 and SQ2 under alternating illumination of blue light (475 nm) and red light (660 nm). (Include the molecular structures of the dyes D5 and SQ2). Adapted from (53) Licensed under an open-access Creative Commons CC BY 4.0 license).

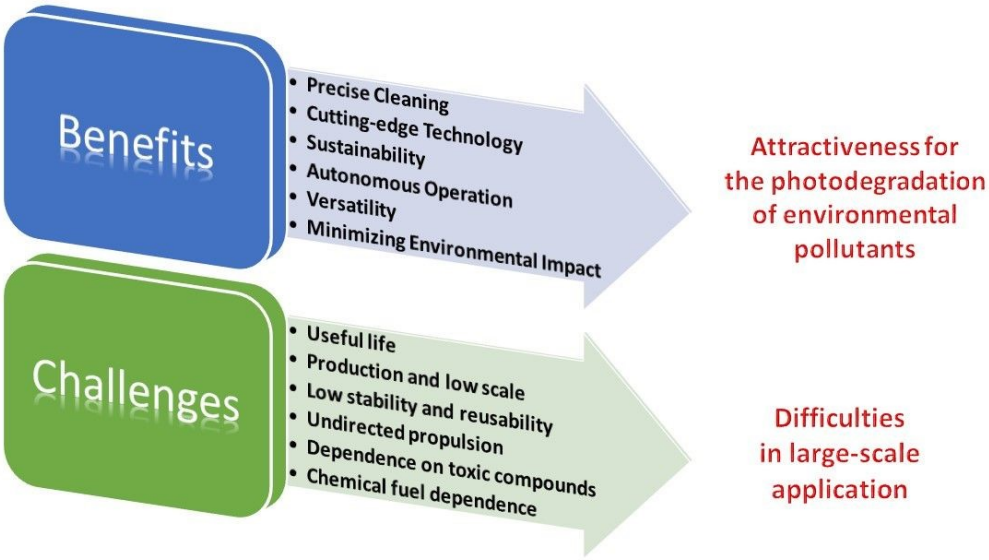

Figure 3. Schematic of the benefits and limitations highlighted until 2020, in the use of photocatalytic Vis-LDM in the degradation of environmental pollutants.

View Article Online
DOI: 10.1039/D4VA00230J

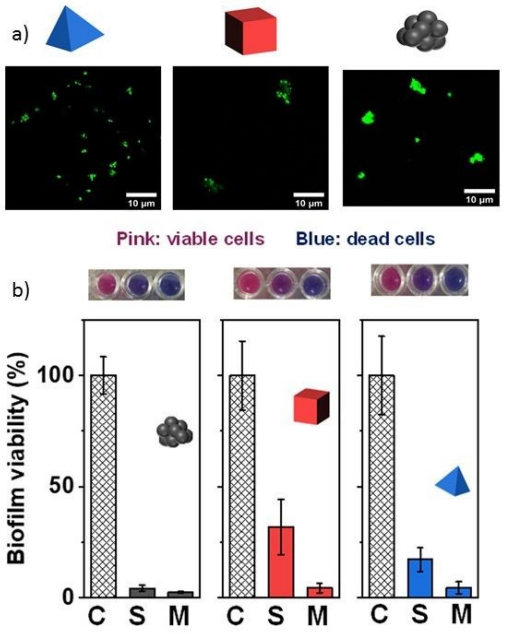

Figure 4. a) Fluorescence microscopy images of Vis-LDM based on Ag_3PO_4 in tetrahedral, cubic, and amorphous forms in pure water under light excitation (λ = 488 nm); b) Effect of Vis-LDM on *methicillin-resistant S.* aureus biofilms under visible light irradiation and in the dark for 60 minutes. C (control): without light irradiation and Vis-LDM, S (static): in the presence of Vis-LDM and M (moving): in the presence of Vis-LDM and light. Adapted from (21) (Licensed under an open-access Creative Commons CC BY 4.0 license).

View Article Online
DOI: 10.1039/D4VA00230J

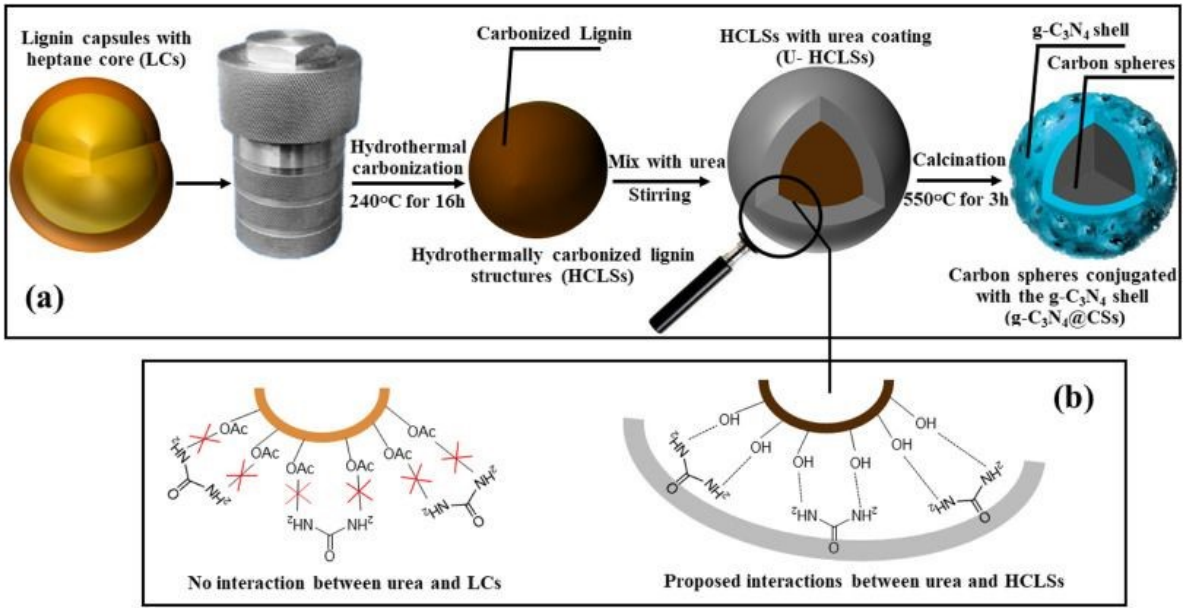

Figure 5. (a) Synthesis scheme of g-C_3N_4@CSs from Kraft lignin and urea. (b) Proposed molecular interactions between urea and the surfaces of CSs (made of acetylated lignin) and urea/HCLSs, with and without the presence of -OH groups on the surfaces of HCLSs. Adapted from (77) (Licensed under an open-access Creative Commons CC BY 4.0 license).

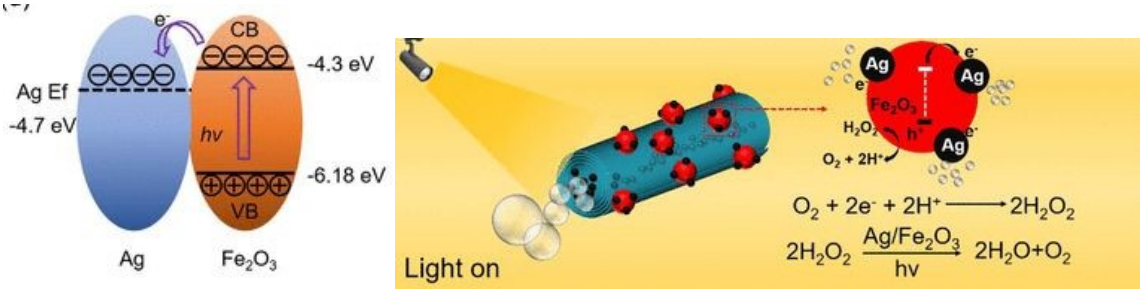

Figure 6. Band structure of the Ag–Fe_2O_3 heterostructure and schematic illustration of a visible light-enhanced propulsion mechanism. Reprinted with permission from (87) (Copyright © 2022 American Chemical Society).

View Article Online
DOI: 10.1039/D4VA00230J

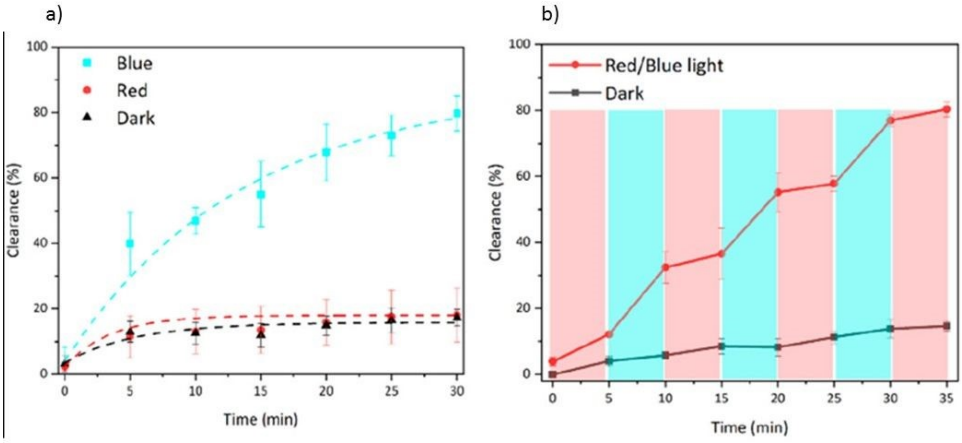

Figure 7. Results of: a) removal of RhB over time by Vis-LDM under blue, red and dark irradiation in a solution containing 50 mM H_2O_2; b) removal of RhB by Vis-LDM under red/blue light switch (5 minutes each, red line) and when kept in the dark (black line). Reprinted with permission from (94) (Copyright © 2023 American Chemical Society).

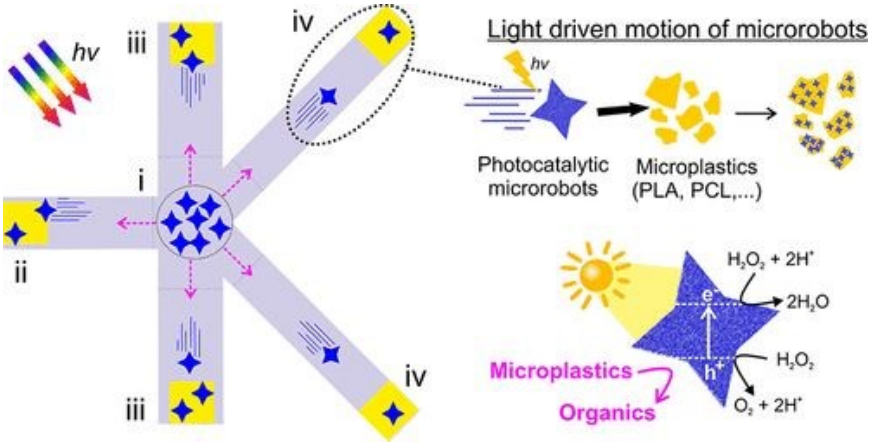

Figure 8. Representative scheme of the autonomous movement, capture, transport and degradation of microplastics by Vis-LDM based on $BiVO_4/Fe_3O_4$ under a solar simulator in a labyrinth with five channels, with lengths of 0.4 cm (ii), 0.6 cm (iii) and 0.8 cm (iv), in the presence of H_2O_2 0.1 % *v/v*. Reprinted with permission from (89) (Copyright © 2021 American Chemical Society).

View Article Online
DOI: 10.1039/D4VA00230J

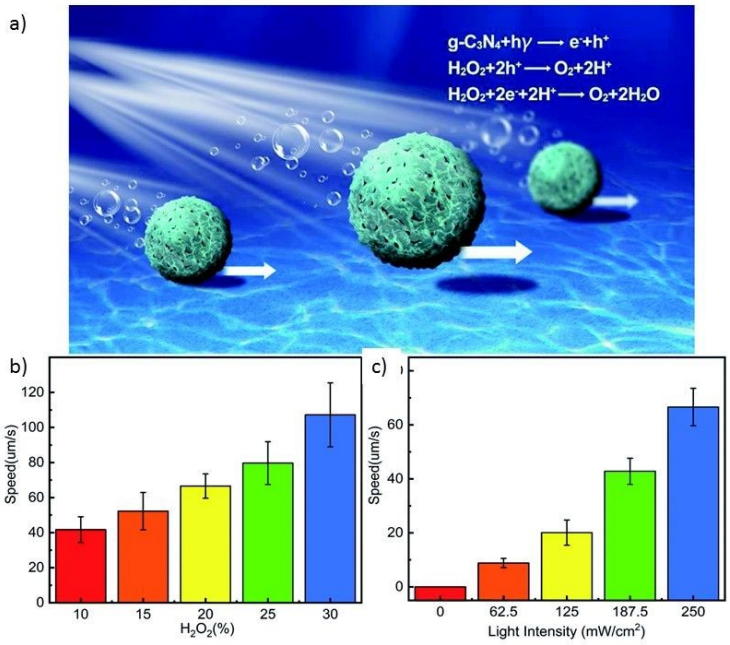

Figure 9. Schematic representation of: (a) the self-propulsion by g-C_3N_4@CMS micromotors; (b) speed of g-C_3N_4@CMS micromotor *versus* H_2O_2 concentration; (c) speed of g-C_3N_4@CMS micromotor *versus* light intensity. Adapted from (30) (Licensed under an open-access Creative Commons CC BY 4.0 license).

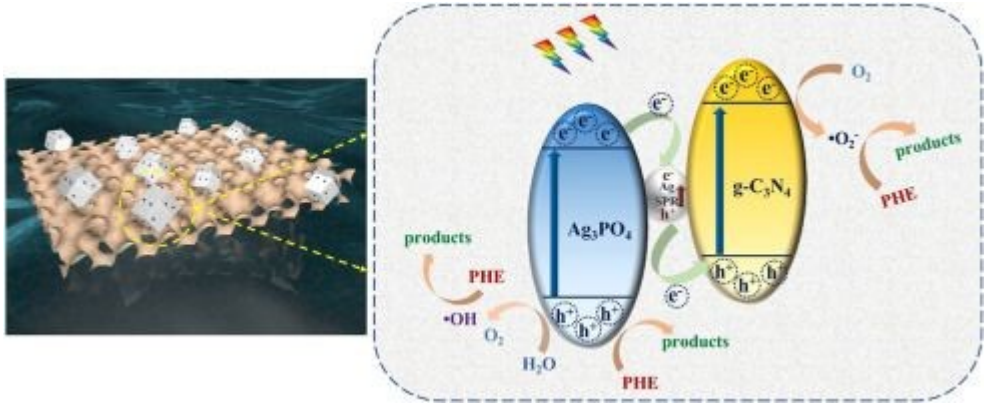

Figure 10. Schematic representation of Vis-LDM based on Ag/Ag_3PO_4/gC_3N_4 with representation charge transfer in a heterostructure. Reprinted with permission from (29) (Copyright © 2022 WILEY-VCH).

View Article Online
DOI: 10.1039/D4VA00230J

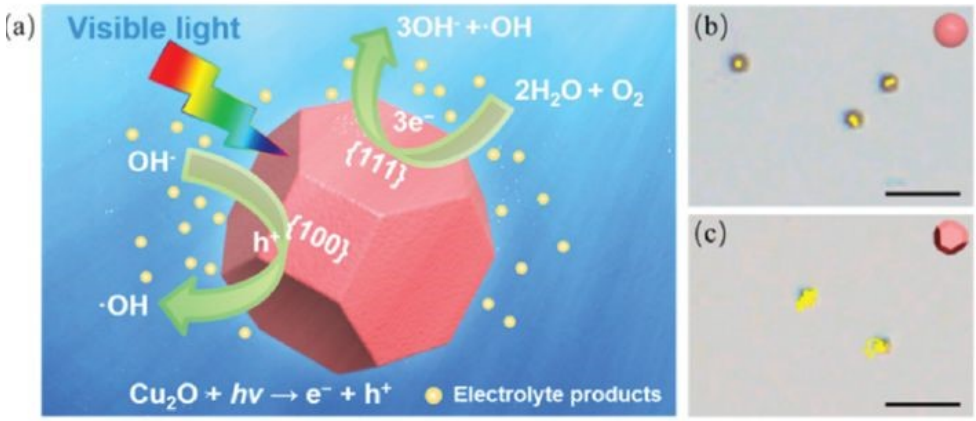

Figure 11. a) Scheme of the propulsion mechanism of a truncated octahedral Vis-LDM based on Cu_2O in pure water under visible light irradiation. (b and c) Motion trajectories of spherical (b) and truncated octahedral (c) Cu_2O motors over 3 seconds. Scale bar: 5 mm. Reprinted with permission from (36) (Copyright © 2021 Royal Society of Chemistry).

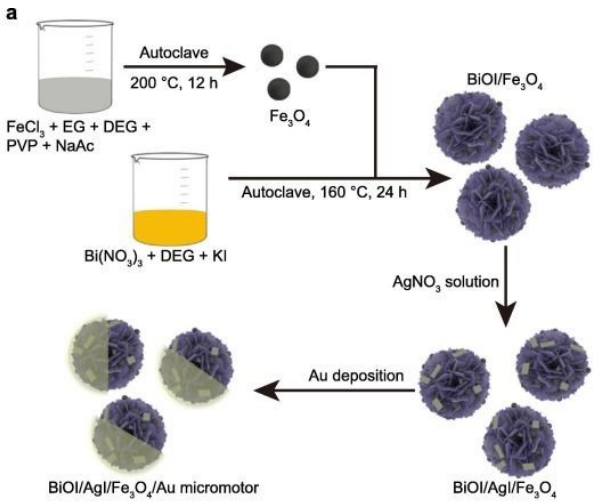

Figure 12. Synthesis scheme of Vis-LDM based on BiOI/AgI/Fe_3O_4 doped with Au. Reprinted with permission from (42) (Copyright © 2020 WILEY-VCH).

View Article Online
DOI: 10.1039/D4VA00230J

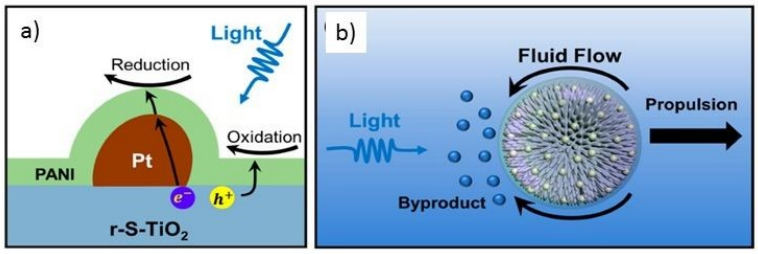

Figure 13. Schematics demonstrating: a) photoelectrochemical reaction that occurs on the surface of the micromotor; b) micromotor propulsion under visible light illumination. Adapted from (92) (Licensed under an open-access Creative Commons CC BY 4.0 license).

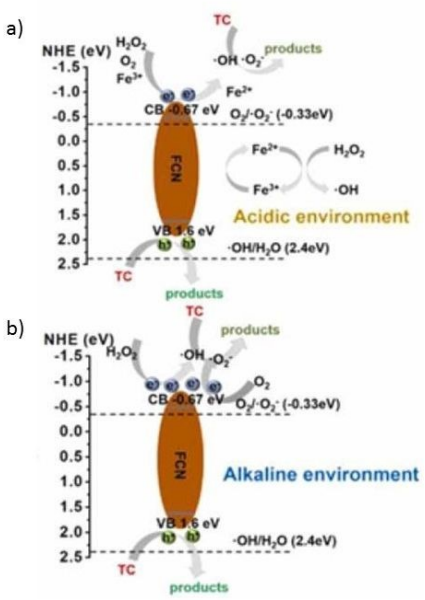

.

Figure 14. Representative scheme of the photodegradation process that occurred: a) in an acidic environment and b) in an alkaline environment. Reprinted with permission from (101) (Copyright © 2022 WILEY-VCH).

View Article Online
DOI: 10.1039/D4VA00230J

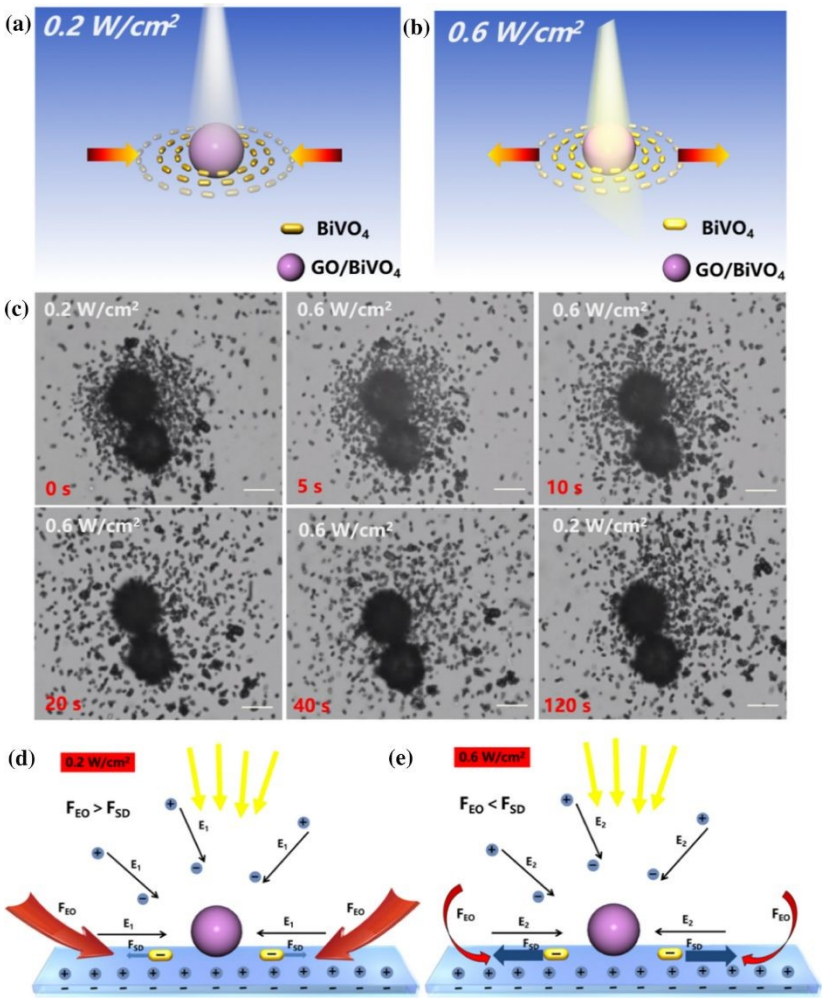

Figure 15. Schematic illustration showing: a,b) the movement of $BiVO_4$ particles around the $GO/BiVO_4$ micromotor under light irradiation of 0.2 Wcm^{-2} and 0.6 Wcm^{-2}, respectively; c) optical microscope images showing the aggregation and disaggregation process of $BiVO_4$ micromotors (scale bar: 5 μm); d,e) Schematic illustration of the aggregation and disassembly behavior and based on the competition between the mechanism of autodiffusiophoresis and electroosmosis, respectively. Adapted from (102) (Licensed under an open-access Creative Commons CC BY 4.0 license).